العنوان:	-Realistic Modeling of Time-Varying MIMO Channel Capacity Using Ray Tracing in Multi-Ring Scattering Environment
المؤلف الرئيسي:	Shtaiwi, Eyad Mahmoud
مؤلفين آخرين:	Harb, Bassam(Advisor)
التاريخ الميلادي:	2015
موقع:	إربد
الصفحات:	1 - 64
رقم MD:	747732
نوع المحتوى:	رسائل جامعية
اللغة:	English
الدرجة العلمية:	رسالة ماجستير
الجامعة:	جامعة اليرموك
الكلية:	كلية الحجاوي للهندسة التكنولوجية
الدولة:	الاردن
قواعد المعلومات:	Dissertations
مواضيع:	أنظمة الاتصالات اللاسلكية
رابط:	https://search.mandumah.com/Record/747732

Chapter 1

INTRODUCTION

1.1 MOTIVATION

WIRELESS Communication systems designers faced new challenges to deal with the increasing demands on high data transfer rates. The need for permanent accessibility and mobility of modern information community over different channel conditions, taking into consideration the limited bandwidth sources. Therefore, the paramount challenges for the next generation(NG) wireless communication systems are to provide mobile broadband data access; i.e. wireless internet access through mobile devices, enhance the overall performance of the system and provide the highest possible quality of service (QoS).

Due to the rapid development in technologies, a new products and services were emerged. For instance, home TV streaming or broadcasting. Such a new service needs 6Mbps to 8Mbps to stream a single video of good quality with MPEG-2 encoded (H.222/H.262). On the other hand, it requires up to 20 Mbps, uninterruptedly and continuously rate, for streaming an MPEG-2 HDTV video. Glance at an existing wireless systems, third-generation (3G) systems provide up to 2Mbps in indoor environments and 144Kbps in outdoor mobile environments; hence current wireless systems are obviously capacity-constrained systems and not applicable for such new applications .

The biggest impediment in the current wireless systems to attain the reliability of the systems over wireless channel is multipath fading, or multipath-induced fading. Multipath fading refers to random fluctuations in the received signal resulting from the large number of different paths between the transmitter and the receiver. Due to the multitude propagation paths , the channel gains and delays of each path are generally different from others. Therefore, the overall received signal is the sum of replicas of transmitted signal and they might be constructively added or destructively subtracted. Such channels in wireless communication systems come from the existence of the obstacles which reflect the transmitted signal and create multiple paths. Time-variant fading channel occurs when transmitter, receiver, and obstacles are moving. Several techniques are used in order to combat multipath fading effects. such as equalization, orthogonal frequency division modulation, Rake receivers, and diversity techniques.

By using multiple antenna elements at either the transmitter or the receiver or at both, multipath is considered as an advantage to significantly boost the system capacity and the reliability. the basic idea behind the use of multiple antennas instead of single antenna is to offer redundancy in signal transmitted over the channel, thus; creating parallel sub-channels over the same used frequency band. Implementation of antenna arrays at the transmitter and/or the receiver exploits multipath propagation environments either to increase the data rate, spectral efficiency of the channel, through spatial multiplexing or to improve the system reliability through antenna diversity.

1.2 MIMO Wireless Communication System

Multiple-Input Multiple-Output, (MIMO), refers to the use of multiple antennas at both the transmitting (Tx) and receiving (Rx) ends as shown in Figure1.1, with the purpose of enhancing the overall system performance. MIMO employs a new dimension called spatial dimension in addition to the natural dimensions, time and frequency, which are used in conventional wireless communication systems [1]. The utilization of antenna arrays at the transmitter; base-station (BS), and the receiver; mobile-station (MS), can be used

either to improve system's reliability, reduce probability of error for realistic systems, or to achieve higher data rate, thus increase spectral efficiency.

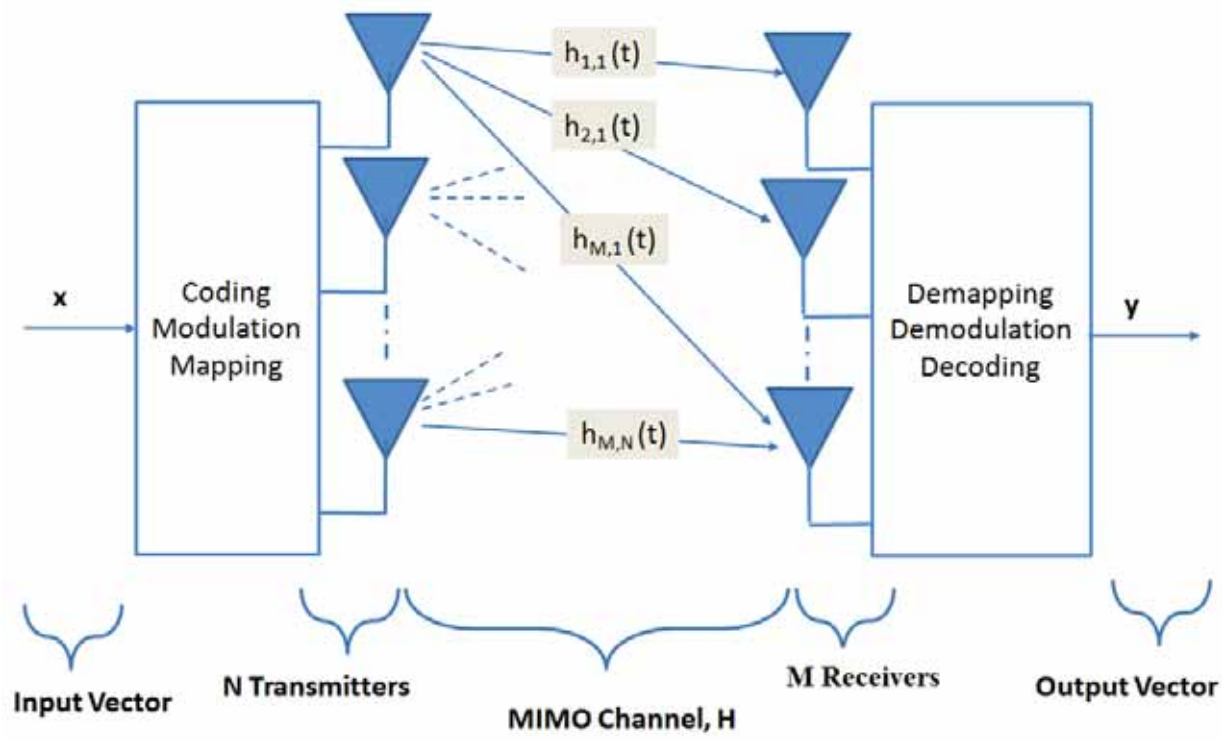

Figure 1.1: Diagram of MIMO Wireless System .

The diversity techniques are used to transmit/receive replicas of the same signal; Hence, the same information are carried through different propagation paths. Spatial diversity, in other words antenna diversity, comes through implementation of multiple antenna elements at the transmitter or/and the receiver. Channel gains between each (Tx-Rx) pair experience certain amount of correlation. The separation between antennas' elements as long as the scatterers' distribution within the environment play a significant role to determine the correlation between channel gains [2] . The required separation depends on the local scattering environment surrounding the transmitter and the receiver [3]. The separation between antenna elements at the receiver to get less independently correlation between each path varies from $0.5\lambda - \lambda$ in general [3]. On the other hand, at the transmitting side the separation ia much greater than that in the receiver.

Spatial diversity techniques are classified into Receiver diversity and transmitter diversity techniques as shown in Figure 1.2. With Receiver diversity antennas' elements are equipped at the receiver. In this case, the system is known to be single- input multiple-output (SIMO). On other hand, transmit diversity techniques use multiple transmit antennas, multiple-input single-output (MISO) system. In addition, multiple-input multiple-output (MIMO) systems provide diversity and even more potentials [1]. Diversity used to combat the fading effects and it helps stabilize the link through channel hardening. Therefore, the probability that all branches are in a deep fade at the same time exponentially reduces with the number of multipaths. The probability that the information is lost due to fading is much reduced, since it would require all branches to fade simultaneously. Hence, this improve the error-performance for wireless communication systems. Space diversity is used in MIMO system where multiple signals that carry the information are transmitted simultaneously over multiple antennas at the same carrier frequency.

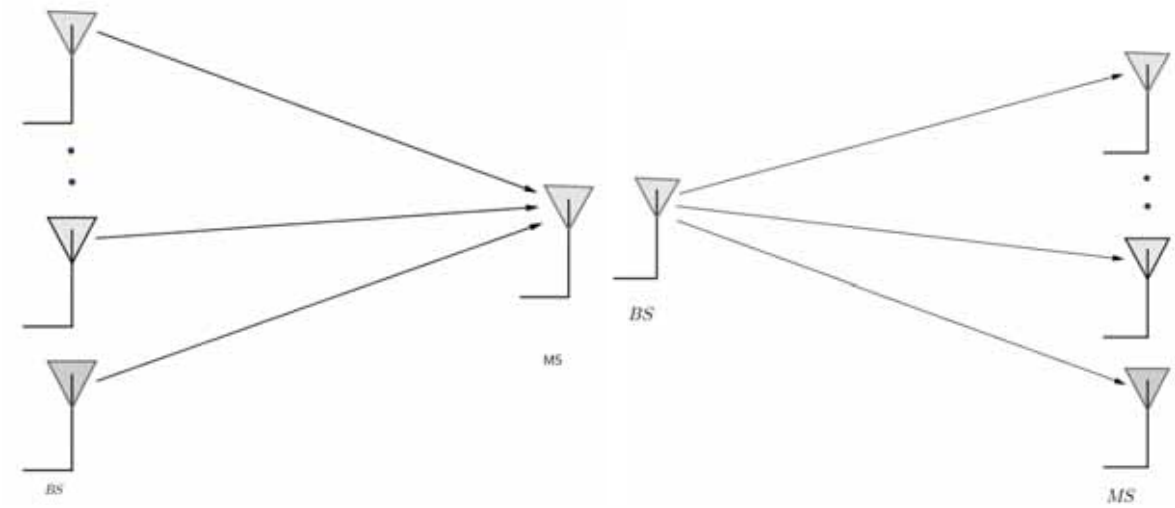

(a) Transmit Diversity *(b) Receive Diversity*

Figure 1.2: Space Diversity Techniques

The promising high spectral efficiency provided by MIMO systems without additional power comes from the fact that MIMO channel can be decomposed into parallel sub-channels or eigenmodes as shown in Figure1.3. The overall capacity of MIMO channel is the sum of the individual capacities provided by the sub-channels. The number of sub-channels, r, is called the rank of MIMO channel matrix, $\mathbf{H}$, [4].

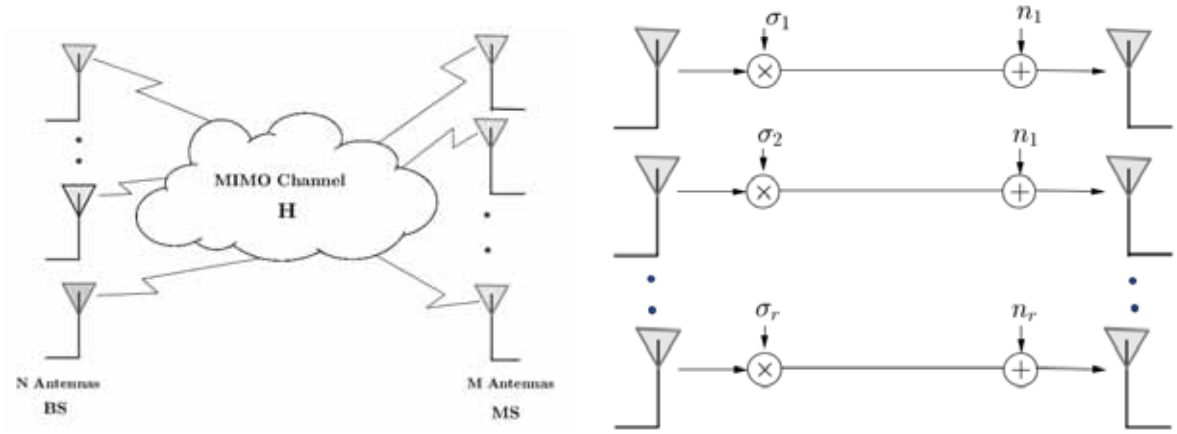

(a) MIMO channel *(b) MIMO channel decomposed into eignmodes*

Figure 1.3: MIMO Channel decomposed into parallel subchannels

The leading feature of MIMO technology is the ability of exploiting multi-paths (spatial dimension), and developing it into a benefit where the signals at the transmitter and the receiver are combined either to improve the bit-error-rate(BER) or to increase the data rate. Therefore, MIMO systems provide a number of solutions to the problems and limitations encountered in the design of communication systems. MIMO system can be used to achieve spatial multiplexing gain, diversity gain, and antenna gain. The benefits of MIMO systems shown in Figure1.4 which include [3]:

- **Spatial multiplexing gain** is defined as the number of the independent streams that can be transmitted simultaneously in order to achieve higher bit rates, without requiring extra bandwidth or extra transmission power [5].

- **Diversity gain** is defined as the number of independent channels that carry the same information in order to enhance the error performance [4].

- **Antenna gain** enhances the signal-to-noise-plus-interference ratio by increasing the post-processing signal-to-noise ratio (SNR) [4]. Beamforming increases the received power by letting antennas to direct their main beam in appropriate direction to achieve better SNR.

Therefore, the design of MIMO transceivers are classified under one of two algorithms. The first algorithm aims to maximize spatial multiplexing gain at certain fixed BER, which increase transfer rate. The second one is designed to improve the reliability,

maximize diversity gain at given transmission rate [2,4,5]. MIMO systems have been important part of modern wireless communication standards such as IEEE 802.11n (WiFi), IEEE 802.16e(WiMAX) , 4G, 3GPP Long Term Evolution, and HSPA^{+} [5] .

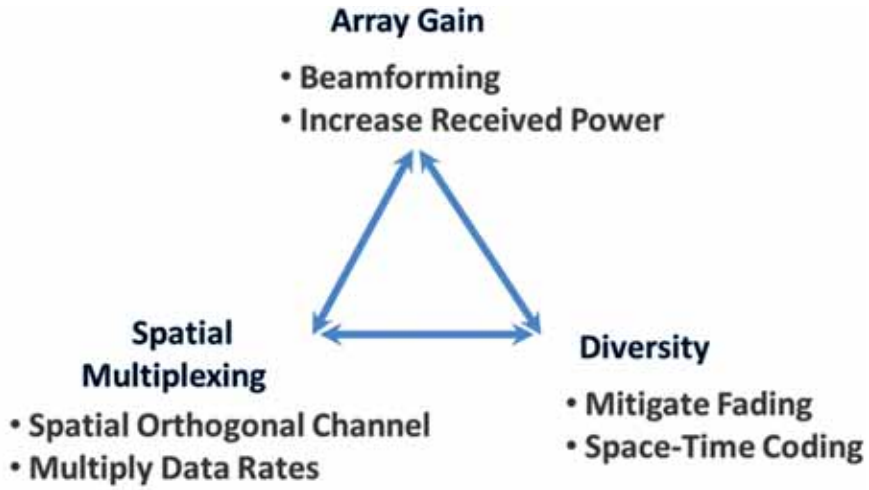

Figure 1.4: Benifits of MIMO Technology

1.3 INFORMATION THEORY RELATED TO MIMO

As we mention before, employment of multiple antennas at both transmitter, or BS, and receiver, or MS, will be used in future wireless communication systems in order to improve quality, capacity, and reliability. So, we need benchmark to study MIMO systems. There are two standpoints to study the performance of these wireless systems. The first perspective, is to evaluate the performance concerning the error probability of the system [6, 7]. The second deals with the evaluation of the information theoretic capacity given by Shannon [8].

Claude Shannon, based on mathematical theory of communications [9, 10], defined channel capacity as the maximum rate that can be achieved for a reliable transmission, arbitrary small error, over the channel without any constraints on complexity of transmitter and receiver [5]. Let C denotes the channel capacity, that's mean for any rate $R < C$ and any probability of error $P_e > 0$ there is a code with rate R that achieves P_e. The length of code and encoding/decoding complexity may be affected by the desired P_e. In other words, the required block length of the code may increase as $P_e \to 0$ and/or $R \to C$. Thus, the capacity is considered as the limit for any wireless communication system.

Channel capacity can be simply expressed in terms of the mutual information between input and output of the channel. So, we need to define the mutual information of wireless channel with random input, $\mathbf{X}$, and random output, $\mathbf{Y}$. The mutual information $I(\mathbf{X};\mathbf{Y})$ is given by [9]:

$$I(X;Y) = H(Y) - H(Y|X) \tag{1.1}$$

The entropy of output $H(Y)$ is given by:

$$H(Y) = -\int f(y) \log f(y) dy \tag{1.2}$$

where the conditional entropy $H(Y|X)$:

$$H(Y|X) = -\int\int f(x,y) \log f(y|x) dx dy \tag{1.3}$$

$$
\begin{aligned}
I(X;Y) &= -\int f(y)\log f(y)dy + \int\int f(x,y)\log f(y|x)dxdy \\
&= -\int\int f(x,y)\log f(y)dxdy + \int\int f(x,y)\log f(y|x)dxdy \\
&= \int\int f(x,y)\log(\tfrac{f(x,y)}{f(x)f(y)})dxdy
\end{aligned} \tag{1.4}
$$

The channel capacity, C, is defined as maximization of mutual information of the channel over all input realizations which is given by [5]:

$$
\begin{aligned}
C &= \max_{f(x)} I(X;Y) \\
&= \max_{f(x)} \int\int f(x,y)\log(\tfrac{f(x,y)}{f(x)f(y)})dxdy
\end{aligned} \tag{1.5}
$$

Equation (1.5) gives general definition for the capacity. So, for additive white Gaussian noise (AWGN) channel the capacity is defined as:

$$
\begin{aligned}
C &= \max_{f(x)} I(X;Y) \\
&= \max_{f(x)} \{H(Y) - H(Y|X)\}
\end{aligned} \tag{1.6}
$$

where $Y = X + n$, X and n are independent. Equation (1.6) becomes:

$$
C = \max_{f(x)} \{H(Y) - H(n)\} \tag{1.7}
$$

where the entropy of Gaussian noise, $n \sim \mathcal{N}(0, \sigma_n)$ is well-known and it is given by:

$$
H(n) = \frac{1}{2}\ln\left(2\pi e\sigma_n^2\right) \tag{1.8}
$$

So, maximizing of equation (1.7) is the input statistics that maximize the output entropy. this can be achieved when the output has a Gaussian distribution which can be obtained when the input also has Gaussian distribution. Therefore, $H(Y)$ is:

$$
H(Y) = \frac{1}{2}\ln\left(2\pi e\left(\sigma_X^2 + \sigma_n^2\right)\right) \tag{1.9}
$$

Thus, the capacity of AWGN channel is given by:

$$\begin{aligned} C &= \tfrac{1}{2}\ln\left(2\pi e\left(\sigma_X^2+\sigma_n^2\right)\right)-\tfrac{1}{2}\ln\left(2\pi e\sigma_n^2\right) \\ &= \tfrac{1}{2}\ln\left(1+\tfrac{\sigma_X^2}{\sigma_n^2}\right) \end{aligned} \tag{1.10}$$

The unit of C in (1.10) is nat per sample. to get the capacity in bit per sec we apply the sampling therom and we should use $\log_2$ instead of ln. For AWGN channel of bandwidth, W, the capacity, in bps, is given by:

$$C = W\log_2(1+SNR) \tag{1.11}$$

Where SNR represents the receive signal-to-noise ratio which is equivalent to the ratio of the variances of signal and noise. The mutual information and entropy in the case where the input and the output are vectors, as MIMO systems, are the same as the scalars. Equation (1.11) represents the capacity for time-invariant channel which is different in case of time-varying channel. Channel capacity of time-varying channel has different definitions. Next, the capacity for single-input single-output(SISO) channel will be found, see Figure 1.5.

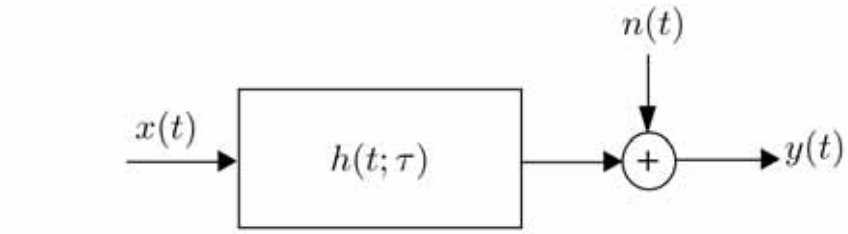

Figure 1.5: Time-varying Single-Input Single-Output(SISO) channel

The Input-Output (I/O) relationship for SISO system can be written as [11]:

$$\begin{aligned} y(t) &= x(t)*h(t;\tau)+n(t) \\ &= \int h(t;\tau)x(t-\tau)d\tau+n(t) \end{aligned} \tag{1.12}$$

Where: $y(t)$ is the system output, $x(t)$ is the system input, $h(t;\tau)$ is the impulse re-

sponse of the channel, and $n(t)$ is the additive white Gaussian noise. For time-selective flat-fading, *non-frequency-selective*, channel the impulse response expressed as:

$$h(t;\tau) = h(t)\delta(\tau) \tag{1.13}$$

Then equation (1.12) becomes:

$$y(t) = h(t)x(t) + n(t) \tag{1.14}$$

For a block of T-symbol length, the output vector $\mathbf{y}$ and input vector $\mathbf{x}$ are described as: $\mathbf{y} = [\ y_1\ y_2\ \cdots\ y_T\ ]$ and $\mathbf{x} = [\ x_1\ x_2\ \cdots\ x_T\ ]$ and the channel gains vector: $\mathbf{h} = [\ h_1\ h_2\ \cdots\ h_T\ ]$. Then, the ergodic capacity of a SISO system can be written as:

$$C_{erg} = E_{\mathbf{h}} log_2(1 + \mathrm{SNR}|\mathbf{h}|^2) \tag{1.15}$$

where $E_{\mathbf{h}}$ is the expected value.

Equation (1.15) defines ergodic capacity, the maximum mutual information averaged over all channel realizations, for SISO system. Outage capacity is defined as the maximum data rate that can be transmitted over the channel with non-zero probability of error. The mathematical definitions for ergodic and outage capacities for MIMO are defined next. Ergodic capacity is used to describe the capacity in fast fading channels. On the other hand, the Outage Capacity is used to characterize the outage probability with any channel rate in slow fading channels [5].

As in the case of SISO system, the input/output relation for MIMO system can be viewed as multi- SISO systems. So, The received signal at i^{th} antenna is denoted by $y_i(t)$ and is expressed as [11]:

$$\begin{aligned} y_i(t) \quad = \quad & \int h_{i1}(t;\tau)x_1(t-\tau)d\tau + \int h_{i2}(t;\tau)x_2(t-\tau)d\tau + \\ & \ldots + \int h_{iN}(t;\tau)x_N(t-\tau)d\tau + n_i(t) \end{aligned} \tag{1.16}$$

$\mathbf{x} : \mathbf{x}(t) = [\ x_1(t)\ x_2(t)\ \cdots\ x_N(t)\ ]^t$represents input vector which includes N transmitted

signals from the BS. The received vector $\mathbf{y} : \mathbf{y}(t) = [\ y_1(t)\ y_2(t)\ \cdots\ y_M(t)\ ]^t$ includes M received signals where $[.]^t$ indicates matrix transpose.

For non-frequency-selective, flat fading channel, the channel impulse response, $h_{ij}(t;\tau) = h_{ij}(t)\delta(\tau)$. So, equation (1.16) can be written as [11]:

$$\begin{aligned} y_i(t) &= h_{i1}(t)x_1(t) + h_{i2}(t)x_2(t) + \\ &\quad \ldots + h_{iN}(t)x_N(t) + n_i(t) \end{aligned} \tag{1.17}$$

where $h_{mn}(t)$is the channel gain between m^{th} receiver element and n^{th} transmitter element. Use matrix notation, the MIMO system based on (1.17) is expressed as:

$$\begin{bmatrix} y_1(t) \\ y_2(t) \\ . \\ . \\ y_N(t) \end{bmatrix} = \begin{bmatrix} h_{11}(t) & h_{12}(t) & .... & h_{1N}(t) \\ h_{21}(t) & h_{22}(t) & .... & h_{2N}(t) \\ . & . & .... & . \\ . & . & .... & . \\ h_{M1}(t) & h_{M2}(t) & .... & h_{MN}(t) \end{bmatrix} \begin{bmatrix} x_1(t) \\ x_2(t) \\ . \\ . \\ x_M(t) \end{bmatrix} + \begin{bmatrix} n_1(t) \\ n_2(t) \\ . \\ . \\ n_M(t) \end{bmatrix} \tag{1.18}$$

Simply, (1.18) can be written as:

$$\mathbf{y}(t) = \mathbf{H}(t)\mathbf{x}(t) + \mathbf{n}(t) \tag{1.19}$$

where $\mathbf{H}(t)$ is the channel gains matrix. and $\mathbf{n} \sim \mathcal{CN}(0, I_N)$, is $N \times 1$ matrix represents the noise term which is assumed to be complex zero-mean Gaussian random process.

For flat-fading MIMO channel, the capacity of the time-varying channel is defined as the sum of capacities of sub-channels averaged over time only. Consider a T-symbol block, the output and input vectors, respectively, are given by [12]:

$$\mathbf{y} = [\ \mathbf{y_1}\ \mathbf{y_2}\ \cdots\ \mathbf{y_T}\ ] \tag{1.20}$$

$$\mathbf{x} = [\ \mathbf{x_1}\ \mathbf{x_2}\ \cdots\ \mathbf{x_T}\ ] \tag{1.21}$$

And the channel matrices can be expressed as:

$$\mathbf{H} = [\ \mathbf{H_1}\ \mathbf{H_2}\ \cdots\ \mathbf{H_T}\ ] \tag{1.22}$$

where $\mathbf{H_i}$ is the channel matrix of block i.

The mutual information between the output and the input can be expressed as [12]:

$$\begin{aligned} I(\mathbf{y};\mathbf{x}) &= I(\mathbf{y};\mathbf{x}|\mathbf{H_1},\mathbf{H_2},...,\mathbf{H_T}) \\ &= \mathrm{E}_{\mathbf{H_1},\mathbf{H_2},...,\mathbf{H_T}}\left[\sum_{k=1}^{T} I(\mathbf{y_k};\mathbf{x_k}|\mathbf{H_k})\right] \\ &= \mathrm{E}_{\mathbf{H_1},\mathbf{H_2},...,\mathbf{H_T}}\sum_{k=1}^{T}\left[log\left(det\left(I+Q\mathbf{H_k}{\mathbf{H_k}}^{\mathcal{H}}\right)\right)\right] \\ &= T\mathrm{E}_{\mathbf{H}}\left[log\left(det\left(I+Q\mathbf{H}\mathbf{H}^{\mathcal{H}}\right)\right)\right] \end{aligned} \tag{1.23}$$

where $[.]^{\mathcal{H}}$ means transpose conjugation operation and $\mathbf{Q}$ is the input covariance matrix. The ergodic capacity for time-varying MIMO channel is obtained by taking time average of (1.23) as [13]:

$$\mathrm{C}_{erg} = E_{\mathbf{H}}\left\{\log\left(\det\left(I+Q\mathbf{H}\mathbf{H}^{\mathcal{H}}\right)\right)\right\} \tag{1.24}$$

where $\mathbf{Q} = \frac{P}{N}\mathbf{I}_N$ in case of uniform power allocation scheme and P is the total transmitted power.

In case of outage capacity, the transmission rate is fixed; say R and the data will not be correctly received if R is greater than the capacity supported by the channel. The outage probability is defined as the probability of incorrect reception [14] and is defined as:

$$\mathcal{P}_{out} = \mathcal{P}\left(\log\left(det\left(I+Q\mathbf{H}\mathbf{H}^{\mathcal{H}}\right)\right) < R\right) \tag{1.25}$$

In general, it is hard to find the capacity for time-varying frequency-selective fading channel. So, the capacity is approximated by dividing up the channel bandwidth(B) into sub-channels with coherence bandwidth and assume the resulting sub-channels are independent, time-varying, and flat-fading channels [13]. Then, the total capacity is the sum of capacities of sub-channels subject to the power constraint averaged over both time and

frequency [13]. Obviously, the capacity of a MIMO channel depends on :

1. The channel averaged SNR .
2. Channel Knowledge,what is known about the channel information at transmitter and receiver sides.
3. The correlation between channel gains on each antenna.

1.4 CHANNEL SIDE INFORMATION

We note that for a time-varying MIMO channel there are different definitions for the capacity which mainly depends on the availability of channel state information or channel distribution at the transmitter and/or the receiver. channel side information can be classified into three main groups as [5]:

Group 1. Perfect Channel State Information at Receiver (CSIR) and perfect Channel State Information at the Transmitter (CSIT). In this case, the transmitter and receiver have instantaneous knowledge about the channel and the transmitter can adapt its transmission strategy (power/rate). Perfect CSIT can be achieved by a feedback link to the transmitter. However, this link may be impaired by noise and due delay which result in degradation of the overall performance of the system.

Group 2. Perfect CSIR and perfect Channel Distribution Information at the Transmitter (CDIT). In this case, the receiver keeps tracking the channel state while transmitter has only information about the distribution of the channel. channel statistics change due the to mobility of environment, the transmitter, the receiver. statistical properties depend on the time interval in which statistics are fed back to the transmitter. in other word, for short-time interval the channel realizations, $\mathbf{H}$, may have non-zero mean and certain correlation between entries that reflect the channel environment. in contrast, for long-time interval the channel matrix, $\mathbf{H}$, may have zero-mean with uncorrelated entries [5, 15] due to averaging over many propagation environments .

Group 3. Channel Distribution Information at the Receiver (CDIR) and CDIT. In this case, the transmitter and receiver have only information about the distribution of the channel.

Group 4. Quantized Channel State Information: In this group, the CSI is assumed to be perfectly known at the receiver. The Receiver feeds $N_B - bit$ quantization of the channel information to the transmitter. It is applicable for slow fading scenarios, where the receiver feeds back quantized information about the channel at the beginning of each block. There are three special models for the distribution of the channel [5]:

(a) Zero-Mean Spatially White (ZMSW) model.

(b) Channel Mean Information (CMI) model.

(c) Channel Covariance Information (CCI) model.

In the three channel models, the channel is modeled as complex Gaussian random variables. The ZMSW model is the most common model for the channel distribution where the channel gains are modeled as Independent and identically distributed (i.i.d), zero-mean, unit variance, complex circularly symmetric Gaussian random variables. Therefore, $\mathbf{H}$ is written as [5]:

$$\mathbf{H} \sim \mathcal{CN}(\mathbf{0}, \mathbf{I}) \tag{1.26}$$

The CMI model is referred to as Mean feedback model where the channel distribution has non-zero mean and white covariance matrix. In this case, the distribution of the channel is described as [5]:

$$\mathbf{H} \sim \mathcal{CN}\left(\mathrm{E}\{\mathbf{H}\}, \sigma^2\mathbf{I}\right) \tag{1.27}$$

In the CCI model, which also known as covariance feedback model, the channel distribution is described as [5]:

$$\mathbf{H} \sim \mathcal{CN}(\mathbf{0}, \Sigma_H) \tag{1.28}$$

Therefore, knowing the channel distribution **H** the channel ergodic capacity is computed using (1.12) and the outage probability is computed using equation (1.13). Therefore different assumptions about the channel distribution will give different capacities for MIMO channel. Thus, the realistic information about the channel gives an accurate capacity evaluation.

In modern wireless systems such as 4 G systems, MIMO technology is used to provide high data rates for mobile users up to hundreds of Mbps. The significance of the thesis comes from the need to know the maximum data rate supported by the channel in the design of MIMO system for 4G systems. Since the main aim of any communication system is to correctly send the data to the receiver, the limit of the transmission rate is important for the proper design of the system and for determining the data rate at which the system should operate. Therefore, the capacity computation will improve the system performance by avoiding transmitting on rates exceed the channel capacity.

1.5 Problem Statement And Thesis Contribution

MIMO methods make use of multi-element antenna arrays at both the transmit and the receive side of a radio link to drastically improve the capacity compare to the traditional single-input single-output (SISO) systems [16] . Theoretical capacity of idealistic channel has been studied in [17–20] in which the classical independent and identically distributed (i.i.d) Rayleigh fading channel is assumed. Independent and identically distributed fades between channel requires sufficient antenna separations and rich scattering environment. They showed that the theoretical information capacity is approximately equal to the minimum number of antenna elements times the capacity of conventional system where the system can provide several independent communication channels between transmitter and receiver. But realistic channel experience lower capacity. Since the correlated signals at the antenna elements lead to a decrease in the capacity [21–23]. Based on an extraction of the parameters of the multipath components. in [23] the authors proved that the capacities are to be about 30% smaller than what would be anticipated from an idealized model .

Assumptions used in literature for evaluation of the capacity in time varying channels are not always realistic since these are based on strong assumptions about the antenna configuration and knowledge about the channel. For example, in [24–26] perfect knowledge of the instantaneous channel information was assumed which is unrealistic in highly mobile channels. this is because of the transmitter may get inaccurate instantaneous information about the channel due to the delay and noise in the feedback link to the transmitter. In [27–29], capacity is computed based on knowledge about channel mean information (CMI). However, CMI reflects outdated channel information and does not take into consideration Doppler spread and the effect of antenna spacing on the correlation between channels.

In this thesis, we present a new approach to evaluate the realistic capacity of time-varying single-user (SU) down-link MIMO channel under average power constraint, using equally power allocation scheme. We describe a unified model for multiple-input multiple output (MIMO) wireless fading channel. This model is more realistic rather than the existing (i.i.d) Rayleigh fading model. that takes into consideration the effect of scattering environment, Doppler spread, and antenna separations. In this thesis, We will answer the following questions:

- What is the effect of antenna separation on the statistical properties of the channel, using the realistic MIMO channel Model?
- What is the preferable antenna separation, at the transmitter and the receiver, will provide less correlation?
- What is the effect of scattering environment, scattering radius and density, on capacity of a MIMO channel?
- Under what conditions high channel capacity can be achieved?
- What is the discrepancy degree between the capacities of the proposed model and Ray-Tracing (RT) simulation?

The rest of this thesis is organized as:Chapter 2 provides related work and literature review on MIMO capacity evaluation. Chapter 3 describes modeling of time-varying MIMO channel in realistic case using space-time covariance and site-specific(ray-tracying) models. In chapter 4, we explain the analysis and simulation results for the capacity of MIMO channel which is modeled in chapter three. Chapter 5 gives conclusions and suggests future work in MIMO capacity modeling and evaluation .

العنوان:	-Realistic Modeling of Time-Varying MIMO Channel Capacity Using Ray Tracing in Multi-Ring Scattering Environment
المؤلف الرئيسي:	Shtaiwi, Eyad Mahmoud
مؤلفين آخرين:	Harb, Bassam(Advisor)
التاريخ الميلادي:	2015
موقع:	إربد
الصفحات:	1 - 64
رقم MD:	747732
نوع المحتوى:	رسائل جامعية
اللغة:	English
الدرجة العلمية:	رسالة ماجستير
الجامعة:	جامعة اليرموك
الكلية:	كلية الحجاوي للهندسة التكنولوجية
الدولة:	الاردن
قواعد المعلومات:	Dissertations
مواضيع:	أنظمة الاتصالات اللاسلكية
رابط:	https://search.mandumah.com/Record/747732

Chapter 2

LITERATURE REVIEW AND RELATED WORK

MIMO communication techniques have the potential for large capacity over traditional SISO systems. The promising high spatial multiplexing gain comes from that MIMO can provide several independent communication channels between transmitter and receiver . In case of ideal multipath propagation channels, MIMO shows linear growth in spectral efficiency. Which open a research area for capacity evaluation of these systems [14].

The capacity of MIMO systems which operate in Rayleigh flat fading is considered under the assumption of perfect channel state information at transmitter and receiver, perfect CSIT and perfect CSIR [24–26]. Based on perfect knowledge of the channel, the transmitter can use optimal power-allocation scheme , water-filling algorithm. Capacity is computed using singular-value decomposition (SVD). The performance of a system using (SVD) over a multiple-input multiple-output MIMO channel is dependent on the accuracy of (CSI) at the transmitter and the receiver It is shown that, large capacity gains are available with optimal power and rate adaptation schemes compared to other cases, such as when there is only channel side information at the receiver. this valid when the instantaneous channel information is available at the receiver and the transmitter; any delayed will cause degradation in the capacity, where perfect CSIT and CSIR can be un-

realistic [5]. However, for a time-varying channel, the availability of accurate CSI at the transmitter is rarely achieved due to an inherent delay between the estimation of the CSI and the transmission of data [30]. It has been well-documented that in realistic scenario MIMO system which has feedback link, the feedback channel may be lossy, distorted by noise, and cause imperfect CSI feedback to the transmitter [31]. The inaccurate CSI may mislead the transmitter to perform the optimal power-allocation [31–34] and such systems employing SVD suffers degradation in capacity when incorrect CSI is used to transmit data.

The authors of [17] compute the capacity of multi-element array systems assuming the channel, **H**, is considered fixed and constant during data transmission . So, there is no need to time-averaging in order to compute channel capacity. The dynamic of local environment and the complexity of scattering; the movement of the mobile station and the scatterers makes the channel varies over time in manner we can't expect [5] . in addition, the channel is assumed to be perfectly known at the transmitter.

They explore the capacity of dual-antenna-array systems [17, 35, 36]. Assume that MIMO wireless systems are using multi-element antenna arrays simultaneously at the both transmitter and receiver with the same size, $p \times p$ MIMO systems. Then, the capacity evaluation is based on assumption that the array size is very large, $p \to \infty$, the asymptotic behaviour of the capacity. The mobile station(MS) is a hand-held device. So, due to physical limitations the size of antenna arrays at MS is restricted and the antennas' elements separation is shorter than that at the base station (BS).

In [17, 37–39] the entries of channel matrix **H** were modeled as independent and identically distributed (i.i.d) complex circularly symmetric Gaussian random variables which gives the higher capacity rather than any other cases when there is no perfect CSIT or CSIR. (i.i.d) Rayleigh fading between channel elements is an idealistic scenario for wireless channel. This assumption requires large number of equally strong paths

with path phases that are uniformly distributed over $[0\ 2\pi]$ which does not always happen [40]. Physical channels, in real, exhibit clustered scattering environments [41] so, the assumption of i.i.d channels are not realistic.

In [36, 42, 43] the authors assumed that the receiver has perfect knowledge about the channel. This assumption requires sending periodic training sequences which comes at the expense of transmission time, which is unrealistic in highly mobile communication systems. Also, they studied the asymptotic behaviour of the capacity.

In [43], the capacity of time-varying channel considered as a random variable. They assumed (i.i.d) Rayleigh fading channel and that the channel is perfectly known at the receiver side. They evaluate the outage probability for the capacity as the number of antennas goes to infinity such that the eigenvalues distribution is well-known when the channel modeled as (i.i.d) Rayleigh channel. Then the capacity distribution of MIMO time-varying channel was derived. The authors in [36] evaluated the capacity of Rayleigh fading MIMO channels considering the capacity gain for general Rayleigh fading channel models. They derived the capacity ratio and the capacity difference relative to the SISO channel at infinite and very low SNRs. evaluation of the capacity at extreme SNR's enabled them to approximate the log-function as linear function.

MIMO channel experiencing correlation between each $(T_x - R_x)$ pair is studied in [17, 44–47]. Where channel correlation is modeled as a separable correlation model, known as Kronecker model. In Kronecker model, the correlation between all possible combinations of the entries in the channel matrix $\mathbf{H}$ is equal to the Kronecker product of the correlation at the transmitter and the receiver. Thus, the correlation, $\mathbf{R} = \mathbf{R}_t \otimes \mathbf{R}_x$. MIMO channel measurements show that the Kronecker model over-perform the realistic MIMO channel capacity [41, 48–50]. Therefore, the need of a realistic model that hopefully estimates the realistic channel capacity. The assumption of zero-mean Rayleigh fading channel is accurate for the channel, $\mathbf{H}$, and it's well-documented [41].

العنوان:	-Realistic Modeling of Time-Varying MIMO Channel Capacity Using Ray Tracing in Multi-Ring Scattering Environment
المؤلف الرئيسي:	Shtaiwi, Eyad Mahmoud
مؤلفين آخرين:	Harb, Bassam(Advisor)
التاريخ الميلادي:	2015
موقع:	إربد
الصفحات:	1 - 64
رقم MD:	747732
نوع المحتوى:	رسائل جامعية
اللغة:	English
الدرجة العلمية:	رسالة ماجستير
الجامعة:	جامعة اليرموك
الكلية:	كلية الحجاوي للهندسة التكنولوجية
الدولة:	الاردن
قواعد المعلومات:	Dissertations
مواضيع:	أنظمة الاتصالات اللاسلكية
رابط:	https://search.mandumah.com/Record/747732

Chapter 3

MIMO SPACE-TIME MODEL

Spatial-temporal (ST) data arises when the data varies across both time and space. Spatial-temporal modeling plays a significant role in modeling mobile wireless channel. Many researches are conducted in spatial and temporal characteristics of wireless channel such Jakes [51], Clarke [52] and others [53]. As we stated before, it has been proven that the model where the channel gains fade as zero-mean Rayleigh distribution is the best for nonline-of-sight (NLS) propagations . In the presence of scatterers, we can assume that the channel gains matrix, $\mathbf{H}$, is modeled as zero-mean with certain covariance matrix, Σ_H. Mathematically, $\mathbf{H} \sim \mathcal{CN}(\mathbf{0}, \Sigma_H)$. Since, it's stated that vectors of Gaussian random variables (real or complex) can be determined by their covariance matrix [54]. In our cases, the covariance matrix is equivalent to the correlation matrix itself, $\Sigma_H = \mathbf{R}$. The correlation between channel gains matrix, $\mathbf{H}$, mainly depends on:

- The scattering environment.
- The antenna separation at T_x and R_x .

For instance, if the majority of channel scatters are located in close proximity to the mobile then the channel gains are highly correlated unless the T_x antennas are sufficiently separated. In some cases, the antennas' elements at transmitting side must be spaced about $(15\lambda - 20\lambda)$ depends on the scattering geometry [17]. The authors in [51, 52] studied scattering models where the scatterers are uniformly distributed on a circular ring with a fixed distance from the mobile station(MS). In [53], circular ring is extended

to deal with multiple-input multiple-output (MISO) systems only. The work [55] examined the effect of fading correlations in MIMO communication systems where the fading statistics determined from the geometrical parameters of the antenna arrays and the multipath propagation environment based on abstract model. But, the Doppler effect wasn't considered, they ignored the motion of the environment. This model is applicable for arbitrary geometry of scattering environment. The geometry of scattering model is shown in Figure 3.1.

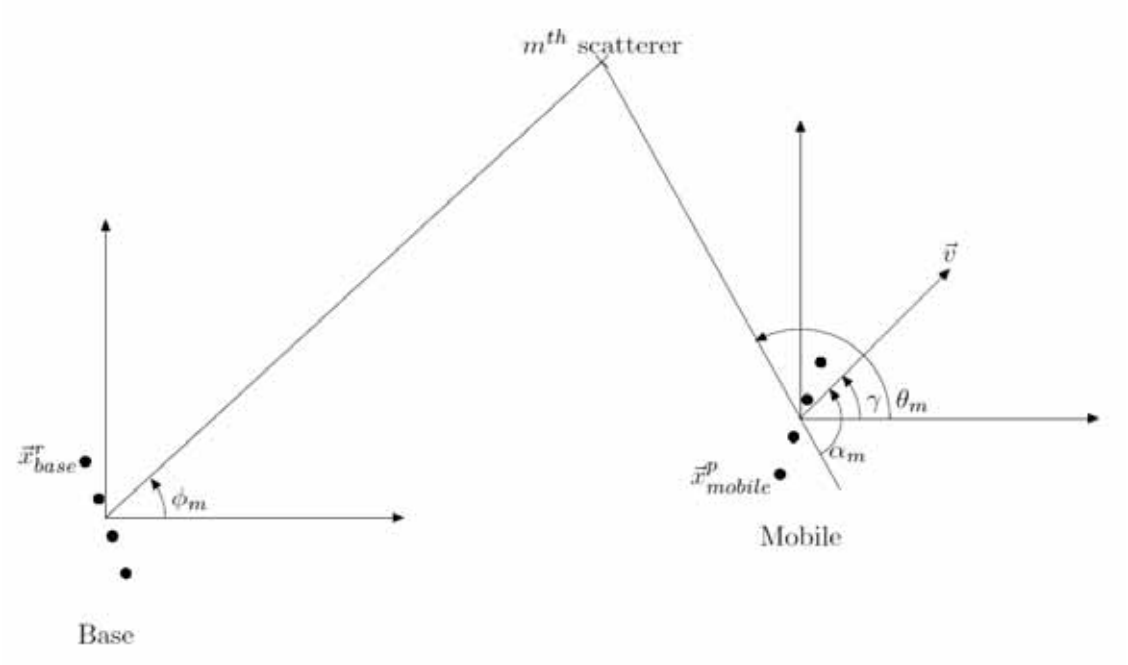

Figure 3.1: Geometry of Scattering Model

Next, we present space-time covariance model of MIMO channel considering scattering environment, physical separations of antenna arrays, and the motion. For system with N transmit antennas and M receive antennas, The output at the m^{th} antenna element is given by :

$$y_m(t) = \sqrt{\frac{\rho}{N}} \sum_{n=1}^{N} h_{nm}(t) x_n(t) + n_m(t) \tag{3.1}$$

Where ρ is the averaged SNR, $x_n(t)$ is the input at the n^{th} antenna element and $n_m(t)$ is the AWGN at the m^{th} output antenna element. and $h_{nm}(t)$ is the complex path gain between

n^{th} transmit element and m^{th} receive element at instant t is given by [56] :

$$h_{m,n}(t) = \sum_{l=1}^{K-1} A_l e^{j\psi_l} e^{-j2\pi f_c \tau_l(t)} e^{j\vec{k}_M^l . \vec{x}_M^m + j\vec{k}_B^l . \vec{x}_B^n} \tag{3.2}$$

where, see Figure 4.1 :

$\tau_l(t)$ is the path delay associated with the l^{th} scatterer.

$\vec{k}_M^l = \frac{2\pi}{\lambda}(\cos\theta_l, \sin\theta_l, 0) = \frac{2\pi}{\lambda}(\cos\theta_l \ \hat{a_x} + \sin\theta_l \ \hat{a_y})$,

θ_l is the Angle-of-Arrival (AoA) at the mobile from the l^{th} scatterer.

$\vec{k}_B^l = \frac{2\pi}{\lambda}(\cos\phi_l, \sin\phi_l, 0) = \frac{2\pi}{\lambda}(\cos\phi_l \ \hat{a_x} + \sin\phi_l \ \hat{a_y})$

ψ_l is the phase associated with the l_{th} scatterer,

λ is the operating wavelength, $\lambda = \frac{c}{f_c}$. f_c is the operating frequency

The phases ψ_l and ψ_s are assumed to be independent ($l \neq s$).

The covariance of MIMO channel is computed as [57]:

$$\Sigma_H = E\{vec(\mathbf{H}) \otimes vec(\mathbf{H}^H)\} \tag{3.3}$$

where: $vec(\mathbf{H})$ is the vector which is formed by stacking each column in matrix $\mathbf{H}$.

After some mathematical manipulation, the space-time correlation is expressed as:

$$\mathrm{E}\{h_{p,r}(t) h_{q,s}^*(t+\Delta t)\} = \mathrm{E}\left\{\sum_{m=0}^{K-1} A_m^2 \, e^{j2\pi f_d \Delta t \cos\alpha_m} e^{\frac{j2\pi d_{rs}}{\lambda}\cos(\phi_m - \gamma_{rs})} \, e^{j\frac{2\pi D_{pq}}{\lambda}\cos(\theta_m - \Gamma_{pq})}\right\} \tag{3.4}$$

See Appendix A for derivation.

We note that the spatio-temporal correlation is function of: antenna spacing at both transmitter, D_{pq}, and receiver, d_{rs}, AoA, AoD, antenna configuration and Doppler spread. Different scenarios give different amount of correlation. We will present a realistic and more general scattering model to compute covariance of MIMO channel which will be used in capacity computation.

3.1 INTEGRATED SCATTERING MODEL

The statistical properties of AoA and AoD are two main factors needed in order to compute the correlation between channel gains. Statistics of AoA and AoD affected by geometric shape of the scattering environment and the distribution of surrounding scatterers within the propagation environment. So, assumptions on the distribution of the scatterers and the shape of the scattering area have a paramount importance in estimating the statistics of AoA and AoD [58]. The uniform ring model, in which the local scatterers are uniformly distributed on a thin ring centered on the MS, The proposed procedure is applied on a reference model for the geometrical one ring scattering model consisting of an infinite number of local scatterers lying on a ring around the mobile station (MS) [59]. Others consider uniform elliptical, Gaussian, conical scattering models has been studied [60–63]. We will present a scattering model which can be used to describe various types of propagation areas such as urban, sub-urban and rural area.

The model which will be employed to compute the spatio-temporal correlation of MIMO fading channel is shown in Figurespt. It is a scattering disk with the following assumptions:

- All rays reached the MS have equal power.
- Single-Bounce scenario is considered, first order reflection.
- All paths are independent.
- Antenna arrays at both the transmitter and receiver are collocated.
- Base-station antenna is elevated.

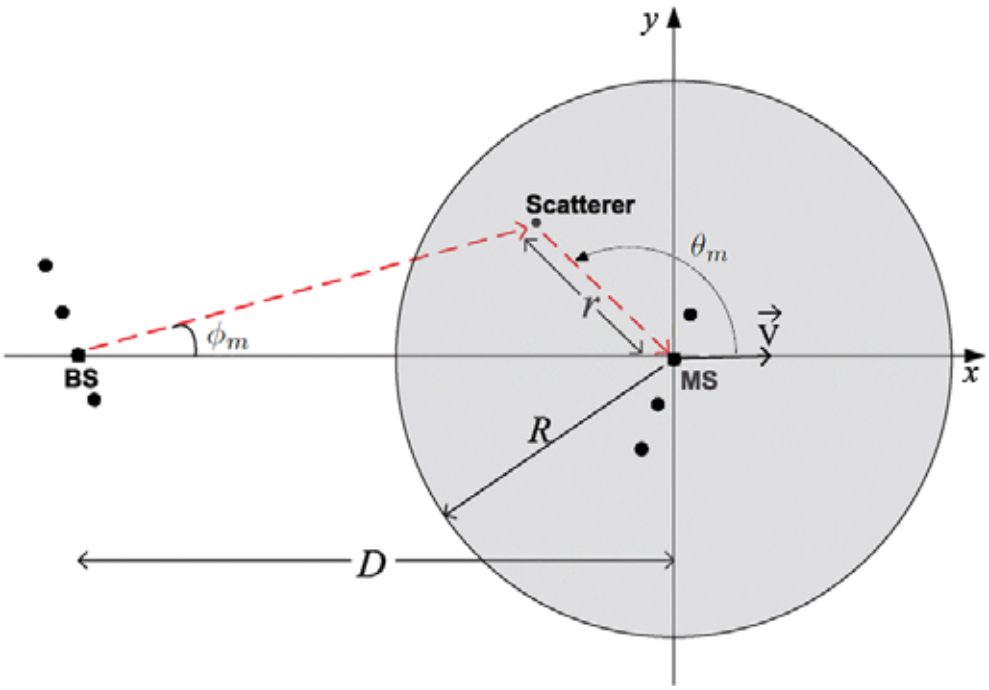

Figure 3.2: Scattering Disk Geometry

Authors in [64] proposed a novel simplistic geometrical disk scattering model in which the local scatterers are uniformly distributed within a disk centred on the mobile station (MS). They expressed the coordination of the local scatterers in polar coordinates, (r, θ_m). The proposed joint uniform distribution results in a higher concentration of scatterers around the disk center and a lower concentration far from it. The joint PDF of local scattering is described as [64] :

$$p_{X,Y}(x,y) = \begin{cases} \frac{1}{2\pi R\sqrt{x^2+y^2}} & \text{,if } x^2+y^2 \leq R^2 \\ 0 & \text{,otherwise} \end{cases} \tag{3.5}$$

Equation 3.5 can be represented in polar coordinates as:

$$p_{r,\theta}(r,\theta) = \begin{cases} \frac{1}{2\pi R} & \text{, } 0 \leq r \leq R, -\pi \leq \theta \leq \pi \\ 0 & \text{, otherwise} \end{cases} \tag{3.6}$$

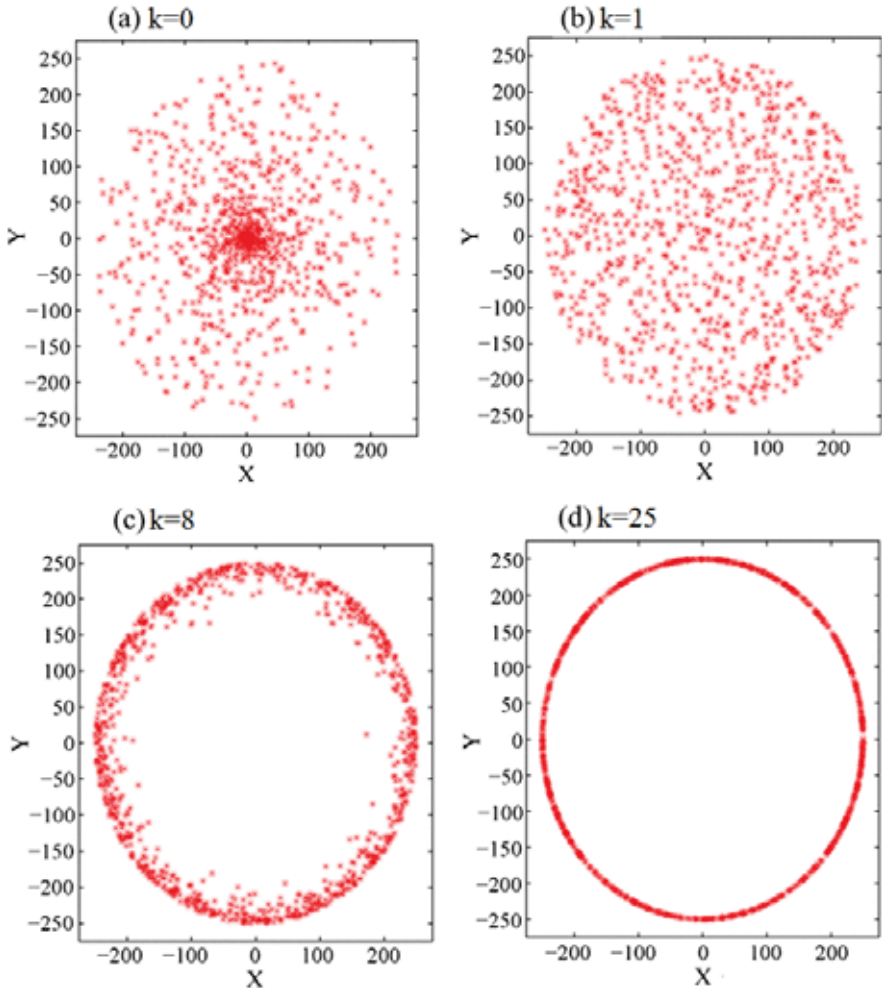

Figure 3.3: Scattering Distributions with different shape factor

Equation 3.6 is clearly independent of r, the joint PDF doesn't depend on the location of local scattering r. That means the effect of the scatter located at radius r and makes angleθ , denoted by S(r,θ) is the same as that located at radius R and makes angle θ , denoted by S(R,θ). Authors in [58] proposed a new model with two degree of freedom, where we can change the radius and the distribution of local scattering. This model can fit real scenarios rather than existing ones. The local scatterers PDF is described as [58]:

$$p_{r,\theta}^{(k)}(r,\theta) = \begin{cases} \frac{(k+1)}{2\pi R^{k+1}} r^k & , 0 \le r \le R, -\pi \le \theta \le \pi \\ 0 & , \text{otherwise} \end{cases} \tag{3.7}$$

Where:

k is called the shape factor. k controls the density of local scatterers around the MS.

R is the radius of local scatterers disk which assumed to be randomly and independently distributed within that disk.

θ is the Angle-of-Arrival of the ray reflected from the scatterer.

D is the distance between the MS and BS.

The model represented in (3.7) is more general model for scattering distribution. Changing the value of k-factor results describing different scattering models. For example, setting $k = 1$ will generate a uniform distribution of the scatterers within a disk around MS. Figure 4.3 demonstrates different situations. For $k = 0$ the scatterers are Gaussian-like distributed, $k = 8$ are hollow-disk. we note that by increasing k the scatterers is distributed over a ring. We will use this model to derive the joint PDF of AoA and AoD required to determine the space-time correlation in Equation (3.4).

The joint PDF of AoA and AoD is given by:

$$p^{(k)}_{\phi,\theta}(\phi,\theta) = \begin{cases} D^{k+1}\frac{(k+1)}{2\pi R^{k+1}}\frac{|\sin(\theta)|\sin^k(\phi)}{\sin^{k+2}(\theta-\phi)} & , (\phi,\theta) \in \mathcal{R} \\ 0 & , \text{otherwise} \end{cases} \tag{3.8}$$

where:

$$\mathcal{R} \in \left\{(\phi,\theta) \mid 0 \leq \frac{D\sin(\phi)}{\sin(\theta-\phi)} \leq R, \theta \neq \phi\right\}$$

See the proof in Appendix B In Figurepdfs, the joint PDF of AoA and AoD for different values of the shape factor k are plotted.

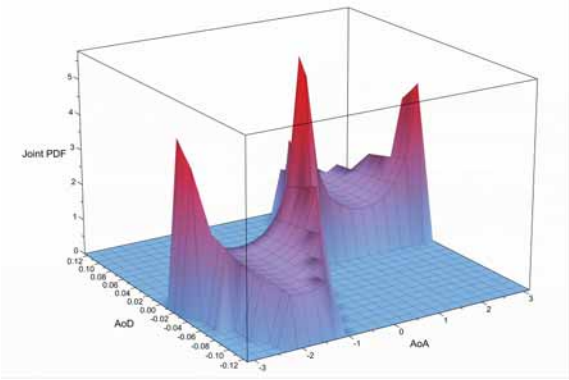

(a) $k = 0$

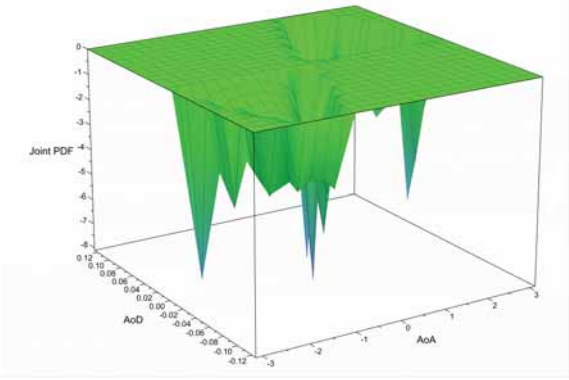

(b) $k = 1$

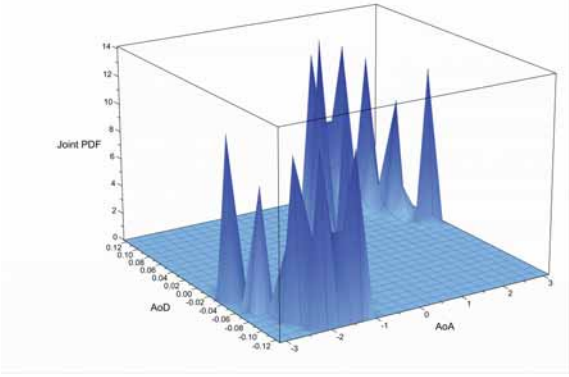

(c) $k = 8$

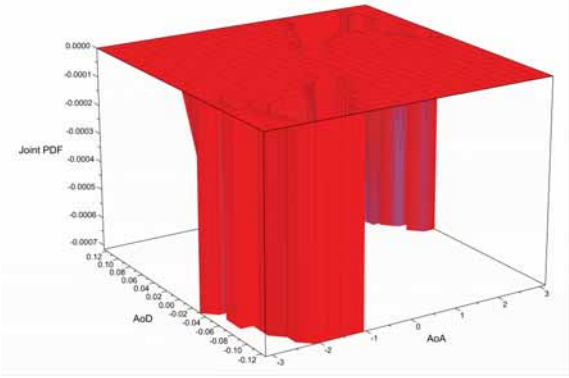

(d) $k = 25$

Figure 3.4: Joint PDF of AoA and AoD for different shape factors k.

3.2 Ray Tracing

Accurate knowledge about the propagation characteristic of the environment need to be known before implementing of wireless system. Propagation prediction is used to anticipate characteristics of channel. The parameters of propagation characteristics without channel prediction techniques can only be estimated by measurements which are time consuming and expensive.

Models used to characterize propagation channels can be divided into three types:

- Empirical Model:

  Based on field measurements, a set of equations derived to describe the propagation characteristics of wireless channels. Empirical models only applicable on environments that have the same characteristics of the channel were measurements are made. So, we cann't use this model to describe different propagation environments without modification.

- Theoretical Model:

  Ideal assumptions are made to estimate the propagation channel charecteristics. Theoretical models are efficient but the assumptions are not always realistic.

- Site-Specific Model:

  Such as Ray-Tracing (RT) method. the propagation environment are input parameter to such method. the input parameter can be very detailed and more accurate describing real channel. RT is used to deal with complex propagation environments. The basic idea behind RT-algorithm is to determine the trajectory of a ray generated from BS and received by MS.

A C++ based simulator, called Ray Tracer (RT), is used in this thesis to verify mathematical results in computing the capacity. RT, developed by Conor Brennan at DCU, finds all possible paths, or rays, between the transmitter and receiver. This is done after inserting the data regarding the location information of the transmitter and the receiver and reading the building data of the surrounding environment of the channel. All possible

rays received at the receiver are calculated using optical theory (based on incident and reflected angles) and creating images for the points of incident.

The electric field of each ray at the receiver is computed using Hertzian dipole or Elementary Doublet method. Assuming the antenna as a small conductor carry current distribution, the electric field is given by:

$$E_\theta = \frac{j(\eta I_0 \delta L)}{4\pi}\left(\frac{k}{r} - \frac{-j}{r^2} - \frac{1}{kr^3}\right) e^{-jkr} sin(\theta) \tag{3.9}$$

Where r is the radial distance between the transmitter and receiver, k is the propagation constant, and θ is the angle between the distance vector, between the transmitter and receiver, and the positive z-axis. Therefore, for each ray at the receiver the received power is computed, the phase, and from the path length the time delay are computed. This information is used to find the channel gains between transmitter and receiver as :

$$h_{mn} = \sum_{i=0}^{M} \sqrt{P_i} e^{j\theta_i} e^{j2\pi f \tau_i} \tag{3.10}$$

Where: M is the total number of rays received at antenna's element. P_i, θ_i, and τ_i are the received power, the phase and the time delay of ith ray,respectively. f is the operating frequency. By using equation (1.27) we can construct the channel gain matrix, **H**. and then compute the capacity of MIMO channel using MATLAB.

العنوان:	-Realistic Modeling of Time-Varying MIMO Channel Capacity Using Ray Tracing in Multi-Ring Scattering Environment
المؤلف الرئيسي:	Shtaiwi, Eyad Mahmoud
مؤلفين آخرين:	Harb, Bassam(Advisor)
التاريخ الميلادي:	2015
موقع:	إربد
الصفحات:	1 - 64
رقم MD:	747732
نوع المحتوى:	رسائل جامعية
اللغة:	English
الدرجة العلمية:	رسالة ماجستير
الجامعة:	جامعة اليرموك
الكلية:	كلية الحجاوي للهندسة التكنولوجية
الدولة:	الاردن
قواعد المعلومات:	Dissertations
مواضيع:	أنظمة الاتصالات اللاسلكية
رابط:	https://search.mandumah.com/Record/747732

Abstract

The use of multiple antenna elements(MAE) at transmitter and receiver increases spectral efficiency of wireless communication channels. This technology is commonly known as MIMO technology. Since the capacity represents the limiting information rate that can be achieved over a channel, it is considered as a benchmark to design any communication system. For time-varying channels, there are two definitions of capacity: ergodic capacity and outage capacity. In this thesis, the ergodic capacity of a time-varying channel is computed by modeling the MIMO channel in more general and realistic scattering model, irrespective to antenna type. Specifically, the time-varying MIMO channel is modeled by geometry-based stochastic (GSC) model. Using GSC model, we compute spatial-temporal correlation while considering the antenna spacing between array's elements, Doppler spread, local scatterers and environment as inputs. In addition, we use C++ simulator, called Ray Tracer, to verify the theoretical results and compare it with results obtained from the mathematical calculations of capacity. We also compare the measured capacity under different scenarios of scatterers distribution and density. The measured capacity found to be 30% less than that for the classical channel model; i.e. independently and identical distributed (i.i.d) Rayleigh fading channel. Thus, we need a more realistic channel model to achieve an accurate computation for the capacity provided by the MIMO channel. Simulation results show that for some scenarios where local scatterers are dense around mobile-station the capacity is 90% less than that for i.i.d channels.

الملخص

النمذجة الواقعية لسعة القناة المتغيرة مع الزمن للنظام متعدد المرسلات ومتعدد المستقبلات باستخدام متتبع الأشعة في بيئة التشتت متعددة الحلقات - اياد محمود شتيوي

يعد استخدام الهوائيات متعددة العناصر تكنولوجيا جديدة و معاصرة لتحسين اداء الانظمة اللاسلكية الموجودة. تُعرف هذه التكنولوجيا بـالأنظمة متعددة الادخالات و متعددة المخرجات. لتقييم أداة هذه الانظمة الجديدة هناك معيارين: أحدهما يقوم بايجاد معدل الخطأ المعروف بـ (BER), بينما المعيار الثاني يقوم بحساب سعة القناة. تعتبر سعة القناة الحد الاقصى المسموح به للارسال خلال هذه الانظمة. لذلك حتى يتم استقبال البيانات بنسبة خطأ صغيرة نحتاج لمعرفة السعة الحقيقية للقناة.

بالنسبة للقنوات المتغيرة مع الزمن هناك تعريفين للسعة: السعة المتوسطة و السعة مع نسبة الخطأ. تُعبر السعة المتوسطة عن متوسط سعات القنوات لجميع العينات بالنسبة للزمن. أما السعة مع الخطأ نقوم بحساب سعة القناة بوجود نسبة معينة من سماحية الخطأ.

في هذا العمل قمنا بحساب السعة المتوسطة عن طريق نمذجة القناة الواقعية باستخدام نموذج عام و شامل للمشتتات. أخذنا بعين الاعتبارحالات متعددة من توزيعات و كثافات هذه المشتتات بغض النظ عن نوع الهوائي المستخدم. باستخدام النموذج العام للمشتتات اوجدنا الخصائص المتعلقة بالزمن و المكان للقناة. أيضا , قمنا بحساب سعة القناة عن طريق برنامج محاكاة للواقع. و استخدمنا هذا البرنامج للمقارنة بين النتائج التيحصلنا عليها من خلال الخصائص الزمانية و المكانية للقناة. و قمنا كذلك بمقارنة هذه القيم بقناوات مقاسة على ارض الوقع.

اشارت النتائج الى ان هناك تفاوت كبير بين السعة المزودة من القناة المثالية و القنوات المقاسة و النموذج النظري. حيت كانت نسبة الخطأ تصل الى ٣٠% بمقارنة القنوات المقاسة الى المثالية. و كذلك كانت نسبة الخطأ تصل الى أكثر من ٩٠% بمقارنة السعة للقناة النظرية و المثالية.

العنوان:	-Realistic Modeling of Time-Varying MIMO Channel Capacity Using Ray Tracing in Multi-Ring Scattering Environment
المؤلف الرئيسي:	Shtaiwi, Eyad Mahmoud
مؤلفين آخرين:	Harb, Bassam(Advisor)
التاريخ الميلادي:	2015
موقع:	إربد
الصفحات:	1 - 64
رقم MD:	747732
نوع المحتوى:	رسائل جامعية
اللغة:	English
الدرجة العلمية:	رسالة ماجستير
الجامعة:	جامعة اليرموك
الكلية:	كلية الحجاوي للهندسة التكنولوجية
الدولة:	الاردن
قواعد المعلومات:	Dissertations
مواضيع:	أنظمة الاتصالات اللاسلكية
رابط:	https://search.mandumah.com/Record/747732

Contents

List of Tables

List of Figures

العنوان:	-Realistic Modeling of Time-Varying MIMO Channel Capacity Using Ray Tracing in Multi-Ring Scattering Environment
المؤلف الرئيسي:	Shtaiwi, Eyad Mahmoud
مؤلفين آخرين:	Harb, Bassam(Advisor)
التاريخ الميلادي:	2015
موقع:	إربد
الصفحات:	1 - 64
رقم MD:	747732
نوع المحتوى:	رسائل جامعية
اللغة:	English
الدرجة العلمية:	رسالة ماجستير
الجامعة:	جامعة اليرموك
الكلية:	كلية الحجاوي للهندسة التكنولوجية
الدولة:	الاردن
قواعد المعلومات:	Dissertations
مواضيع:	أنظمة الاتصالات اللاسلكية
رابط:	https://search.mandumah.com/Record/747732

YARMOUK UNIVERSITY

HIJJAWI FACULTY FOR ENGINEERING TECHNOLOGY

MASTER THESIS

Realistic Modeling of Time-Varying MIMO Channel Capacity Using Ray-Tracing in Multi-Ring Scattering Environment

Thesis Submitted to:
The Department of Telecommunications Engineering

In partial fulfilment of the requirements
for the degree of Master of Science

By:
EYAD MAHMOUD SHTAIWI
Supervisor:
DR. BASSAM HARB

April 2015

Realistic Modeling of Time-Varying MIMO Channel Capacity Using Ray-Tracing in Multi-Ring Scattering Environment

By

Eyad Mahmoud Ahmad Shtaiwi

Thesis Submitted to In Partial Fulfilment of the Requirements
For the Degree of Master of Science in Electrical Engineering

At

Hijjawi Faculty for Engineering Technology

Yarmouk University

April, 2015

Committee Members	Signature and Date
Dr. Bassam Ahmad Harb (Chairman)	.....
Dr. Haythem Bany Salameh (member)	.....
Dr. Mohammad Banat (member)	.....

DEDICATION

Dedicated to my beloved mother, father, brothers and sisters.

ACKNOWLEDGEMENT

First and foremost, I would like to thank Allah, the Almighty, for having made everything possible by giving me strength and patience to do this work.

I would express a deep sense of gratitude to my parents. who have always stood by me like a pillar in times of need. All the support they have provided me over the years was the greatest gift anyone has ever given me.

I would especially like to thank my thesis advisor, Dr Bassam A. Harb. Dr.Bassam's boundless energy an enthuasiam have been ispiration for me. The support an guidance he has given me during the completion of this thesis are truly appreciated.

Besides my advisor, I would like to express my sincere gratitude to my Dr Khaled Gharaibeh for the continuous support of my study and research, for his patience.

Sincere thanks to my brothers, sisters, and all my friend.

Eyad Mahmoud Shtaiwi

Contents

List of Tables

List of Figures

Abstract

The use of multiple antenna elements(MAE) at transmitter and receiver increases spectral efficiency of wireless communication channels. This technology is commonly known as MIMO technology. Since the capacity represents the limiting information rate that can be achieved over a channel, it is considered as a benchmark to design any communication system. For time-varying channels, there are two definitions of capacity: ergodic capacity and outage capacity. In this thesis, the ergodic capacity of a time-varying channel is computed by modeling the MIMO channel in more general and realistic scattering model, irrespective to antenna type. Specifically, the time-varying MIMO channel is modeled by geometry-based stochastic (GSC) model. Using GSC model, we compute spatial-temporal correlation while considering the antenna spacing between array's elements, Doppler spread, local scatterers and environment as inputs. In addition, we use C++ simulator, called Ray Tracer, to verify the theoretical results and compare it with results obtained from the mathematical calculations of capacity. We also compare the measured capacity under different scenarios of scatterers distribution and density. The measured capacity found to be 30% less than that for the classical channel model; i.e. independently and identical distributed (i.i.d) Rayleigh fading channel. Thus, we need a more realistic channel model to achieve an accurate computation for the capacity provided by the MIMO channel. Simulation results show that for some scenarios where local scatterers are dense around mobile-station the capacity is 90% less than that for i.i.d channels.

Chapter 1

INTRODUCTION

1.1 MOTIVATION

WIRELESS Communication systems designers faced new challenges to deal with the increasing demands on high data transfer rates. The need for permanent accessibility and mobility of modern information community over different channel conditions, taking into consideration the limited bandwidth sources. Therefore, the paramount challenges for the next generation(NG) wireless communication systems are to provide mobile broadband data access; i.e. wireless internet access through mobile devices, enhance the overall performance of the system and provide the highest possible quality of service (QoS).

Due to the rapid development in technologies, a new products and services were emerged. For instance, home TV streaming or broadcasting. Such a new service needs 6Mbps to 8Mbps to stream a single video of good quality with MPEG-2 encoded (H.222/H.262). On the other hand, it requires up to 20 Mbps, uninterruptedly and continuously rate, for streaming an MPEG-2 HDTV video. Glance at an existing wireless systems, third-generation (3G) systems provide up to 2Mbps in indoor environments and 144Kbps in outdoor mobile environments; hence current wireless systems are obviously capacity-constrained systems and not applicable for such new applications .

The biggest impediment in the current wireless systems to attain the reliability of the systems over wireless channel is multipath fading, or multipath-induced fading. Multipath fading refers to random fluctuations in the received signal resulting from the large number of different paths between the transmitter and the receiver. Due to the multitude propagation paths , the channel gains and delays of each path are generally different from others. Therefore, the overall received signal is the sum of replicas of transmitted signal and they might be constructively added or destructively subtracted. Such channels in wireless communication systems come from the existence of the obstacles which reflect the transmitted signal and create multiple paths. Time-variant fading channel occurs when transmitter, receiver, and obstacles are moving. Several techniques are used in order to combat multipath fading effects. such as equalization, orthogonal frequency division modulation, Rake receivers, and diversity techniques.

By using multiple antenna elements at either the transmitter or the receiver or at both, multipath is considered as an advantage to significantly boost the system capacity and the reliability. the basic idea behind the use of multiple antennas instead of single antenna is to offer redundancy in signal transmitted over the channel, thus; creating parallel sub-channels over the same used frequency band. Implementation of antenna arrays at the transmitter and/or the receiver exploits multipath propagation environments either to increase the data rate, spectral efficiency of the channel, through spatial multiplexing or to improve the system reliability through antenna diversity.

1.2 MIMO Wireless Communication System

Multiple-Input Multiple-Output, (MIMO), refers to the use of multiple antennas at both the transmitting (Tx) and receiving (Rx) ends as shown in Figure1.1, with the purpose of enhancing the overall system performance. MIMO employs a new dimension called spatial dimension in addition to the natural dimensions, time and frequency, which are used in conventional wireless communication systems [1]. The utilization of antenna arrays at the transmitter; base-station (BS), and the receiver; mobile-station (MS), can be used

either to improve system's reliability, reduce probability of error for realistic systems, or to achieve higher data rate, thus increase spectral efficiency.

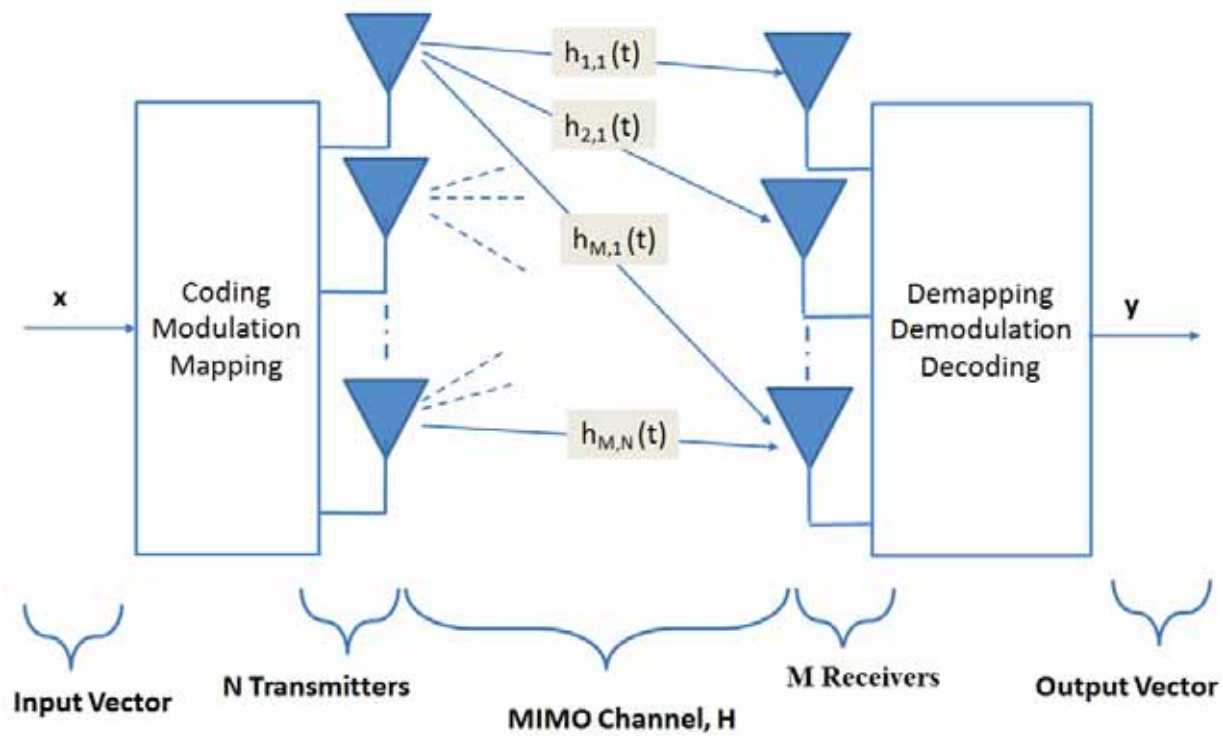

Figure 1.1: Diagram of MIMO Wireless System .

The diversity techniques are used to transmit/receive replicas of the same signal; Hence, the same information are carried through different propagation paths. Spatial diversity, in other words antenna diversity, comes through implementation of multiple antenna elements at the transmitter or/and the receiver. Channel gains between each (Tx-Rx) pair experience certain amount of correlation. The separation between antennas' elements as long as the scatterers' distribution within the environment play a significant role to determine the correlation between channel gains [2] . The required separation depends on the local scattering environment surrounding the transmitter and the receiver [3]. The separation between antenna elements at the receiver to get less independently correlation between each path varies from $0.5\lambda - \lambda$ in general [3]. On the other hand, at the transmitting side the separation ia much greater than that in the receiver.

Spatial diversity techniques are classified into Receiver diversity and transmitter diversity techniques as shown in Figure 1.2. With Receiver diversity antennas' elements are equipped at the receiver. In this case, the system is known to be single- input multiple-output (SIMO). On other hand, transmit diversity techniques use multiple transmit antennas, multiple-input single-output (MISO) system. In addition, multiple-input multiple-output (MIMO) systems provide diversity and even more potentials [1]. Diversity used to combat the fading effects and it helps stabilize the link through channel hardening. Therefore, the probability that all branches are in a deep fade at the same time exponentially reduces with the number of multipaths. The probability that the information is lost due to fading is much reduced, since it would require all branches to fade simultaneously. Hence, this improve the error-performance for wireless communication systems. Space diversity is used in MIMO system where multiple signals that carry the information are transmitted simultaneously over multiple antennas at the same carrier frequency.

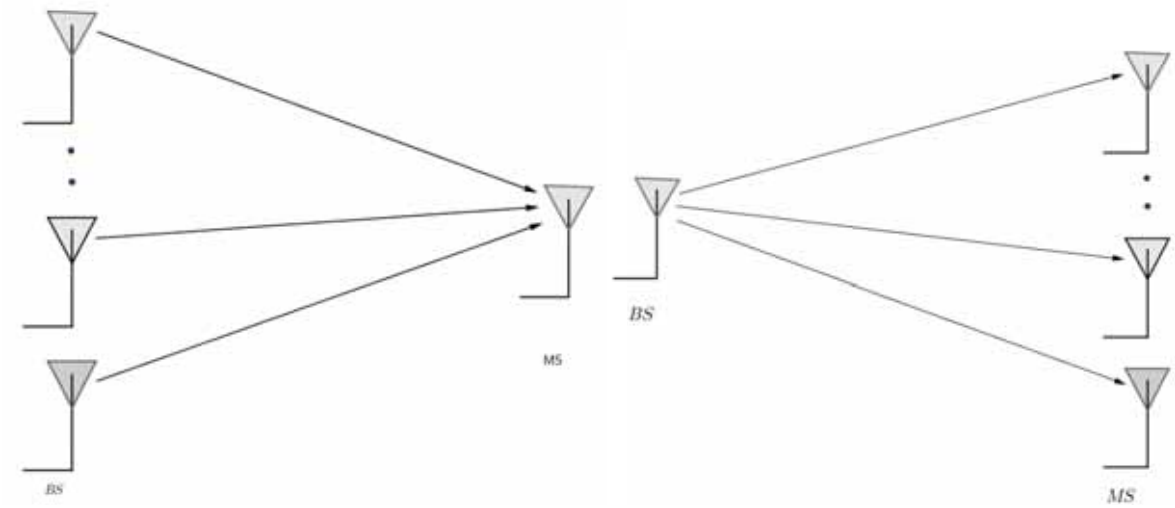

(a) Transmit Diversity *(b) Receive Diversity*

Figure 1.2: Space Diversity Techniques

The promising high spectral efficiency provided by MIMO systems without additional power comes from the fact that MIMO channel can be decomposed into parallel sub-channels or eigenmodes as shown in Figure1.3. The overall capacity of MIMO channel is the sum of the individual capacities provided by the sub-channels. The number of sub-channels, r, is called the rank of MIMO channel matrix, $\mathbf{H}$, [4].

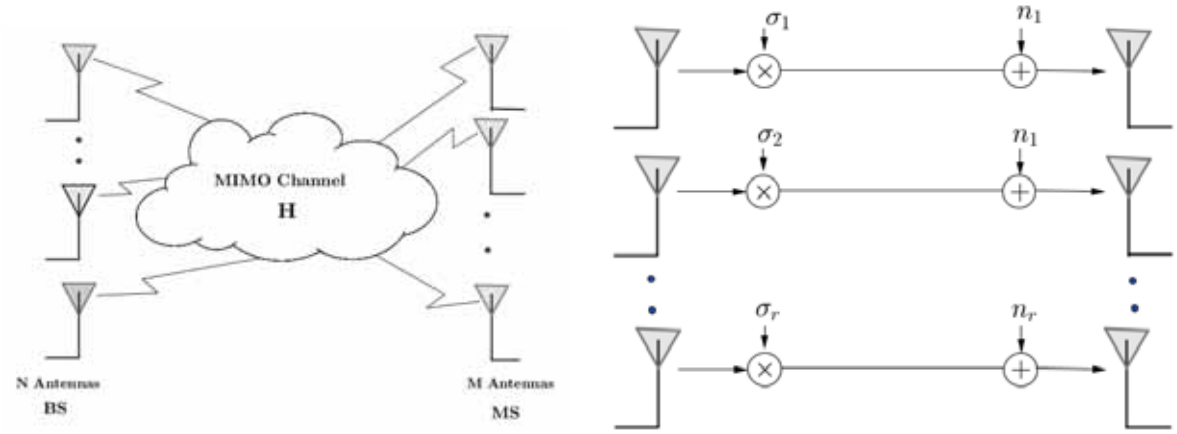

(a) MIMO channel *(b) MIMO channel decomposed into eignmodes*

Figure 1.3: MIMO Channel decomposed into parallel subchannels

The leading feature of MIMO technology is the ability of exploiting multi-paths (spatial dimension), and developing it into a benefit where the signals at the transmitter and the receiver are combined either to improve the bit-error-rate(BER) or to increase the data rate. Therefore, MIMO systems provide a number of solutions to the problems and limitations encountered in the design of communication systems. MIMO system can be used to achieve spatial multiplexing gain, diversity gain, and antenna gain. The benefits of MIMO systems shown in Figure1.4 which include [3]:

- **Spatial multiplexing gain** is defined as the number of the independent streams that can be transmitted simultaneously in order to achieve higher bit rates, without requiring extra bandwidth or extra transmission power [5].

- **Diversity gain** is defined as the number of independent channels that carry the same information in order to enhance the error performance [4].

- **Antenna gain** enhances the signal-to-noise-plus-interference ratio by increasing the post-processing signal-to-noise ratio (SNR) [4]. Beamforming increases the received power by letting antennas to direct their main beam in appropriate direction to achieve better SNR.

Therefore, the design of MIMO transceivers are classified under one of two algorithms. The first algorithm aims to maximize spatial multiplexing gain at certain fixed BER, which increase transfer rate. The second one is designed to improve the reliability,

maximize diversity gain at given transmission rate [2,4,5]. MIMO systems have been important part of modern wireless communication standards such as IEEE 802.11n (WiFi), IEEE 802.16e(WiMAX) , 4G, 3GPP Long Term Evolution, and HSPA^{+} [5] .

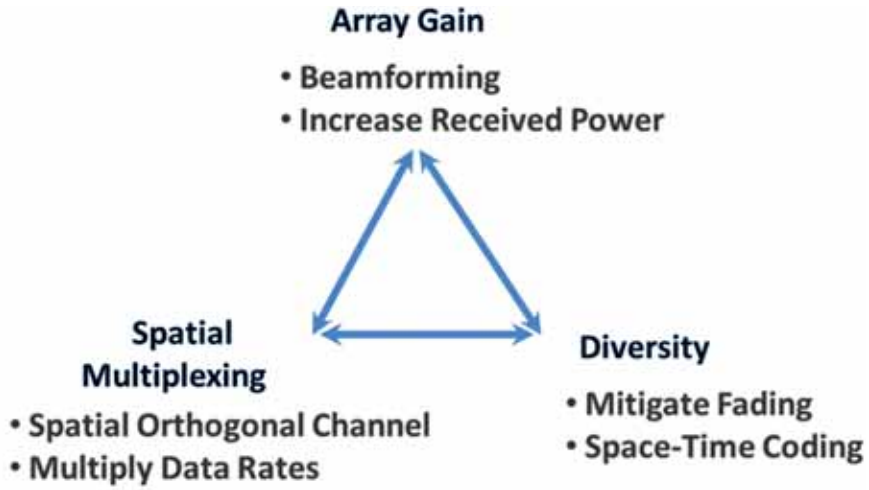

Figure 1.4: Benifits of MIMO Technology

1.3 INFORMATION THEORY RELATED TO MIMO

As we mention before, employment of multiple antennas at both transmitter, or BS, and receiver, or MS, will be used in future wireless communication systems in order to improve quality, capacity, and reliability. So, we need benchmark to study MIMO systems. There are two standpoints to study the performance of these wireless systems. The first perspective, is to evaluate the performance concerning the error probability of the system [6, 7]. The second deals with the evaluation of the information theoretic capacity given by Shannon [8].

Claude Shannon, based on mathematical theory of communications [9, 10], defined channel capacity as the maximum rate that can be achieved for a reliable transmission, arbitrary small error, over the channel without any constraints on complexity of transmitter and receiver [5]. Let C denotes the channel capacity, that's mean for any rate $R < C$ and any probability of error $P_e > 0$ there is a code with rate R that achieves P_e. The length of code and encoding/decoding complexity may be affected by the desired P_e. In other words, the required block length of the code may increase as $P_e \to 0$ and/or $R \to C$. Thus, the capacity is considered as the limit for any wireless communication system.

Channel capacity can be simply expressed in terms of the mutual information between input and output of the channel. So, we need to define the mutual information of wireless channel with random input, $\mathbf{X}$, and random output, $\mathbf{Y}$. The mutual information $I(\mathbf{X};\mathbf{Y})$ is given by [9]:

$$I(X;Y) = H(Y) - H(Y|X) \tag{1.1}$$

The entropy of output $H(Y)$ is given by:

$$H(Y) = -\int f(y) \log f(y) dy \tag{1.2}$$

where the conditional entropy $H(Y|X)$:

$$H(Y|X) = -\int\int f(x,y) \log f(y|x) dx dy \tag{1.3}$$

$$
\begin{aligned}
I(X;Y) &= -\int f(y)\log f(y)dy + \int\int f(x,y)\log f(y|x)dxdy \\
&= -\int\int f(x,y)\log f(y)dxdy + \int\int f(x,y)\log f(y|x)dxdy \\
&= \int\int f(x,y)\log(\tfrac{f(x,y)}{f(x)f(y)})dxdy
\end{aligned} \tag{1.4}
$$

The channel capacity, C, is defined as maximization of mutual information of the channel over all input realizations which is given by [5]:

$$
\begin{aligned}
C &= \max_{f(x)} I(X;Y) \\
&= \max_{f(x)} \int\int f(x,y)\log(\tfrac{f(x,y)}{f(x)f(y)})dxdy
\end{aligned} \tag{1.5}
$$

Equation (1.5) gives general definition for the capacity. So, for additive white Gaussian noise (AWGN) channel the capacity is defined as:

$$
\begin{aligned}
C &= \max_{f(x)} I(X;Y) \\
&= \max_{f(x)} \{H(Y) - H(Y|X)\}
\end{aligned} \tag{1.6}
$$

where $Y = X + n$, X and n are independent. Equation (1.6) becomes:

$$
C = \max_{f(x)} \{H(Y) - H(n)\} \tag{1.7}
$$

where the entropy of Gaussian noise, $n \sim \mathcal{N}(0, \sigma_n)$ is well-known and it is given by:

$$
H(n) = \frac{1}{2}\ln\left(2\pi e\sigma_n^2\right) \tag{1.8}
$$

So, maximizing of equation (1.7) is the input statistics that maximize the output entropy. this can be achieved when the output has a Gaussian distribution which can be obtained when the input also has Gaussian distribution. Therefore, $H(Y)$ is:

$$
H(Y) = \frac{1}{2}\ln\left(2\pi e\left(\sigma_X^2 + \sigma_n^2\right)\right) \tag{1.9}
$$

Thus, the capacity of AWGN channel is given by:

$$\begin{aligned} C &= \tfrac{1}{2}\ln\left(2\pi e\left(\sigma_X^2+\sigma_n^2\right)\right)-\tfrac{1}{2}\ln\left(2\pi e\sigma_n^2\right) \\ &= \tfrac{1}{2}\ln\left(1+\tfrac{\sigma_X^2}{\sigma_n^2}\right) \end{aligned} \tag{1.10}$$

The unit of C in (1.10) is nat per sample. to get the capacity in bit per sec we apply the sampling therom and we should use $\log_2$ instead of ln. For AWGN channel of bandwidth, W, the capacity, in bps, is given by:

$$C = W\log_2(1+SNR) \tag{1.11}$$

Where SNR represents the receive signal-to-noise ratio which is equivalent to the ratio of the variances of signal and noise. The mutual information and entropy in the case where the input and the output are vectors, as MIMO systems, are the same as the scalars. Equation (1.11) represents the capacity for time-invariant channel which is different in case of time-varying channel. Channel capacity of time-varying channel has different definitions. Next, the capacity for single-input single-output(SISO) channel will be found, see Figure 1.5.

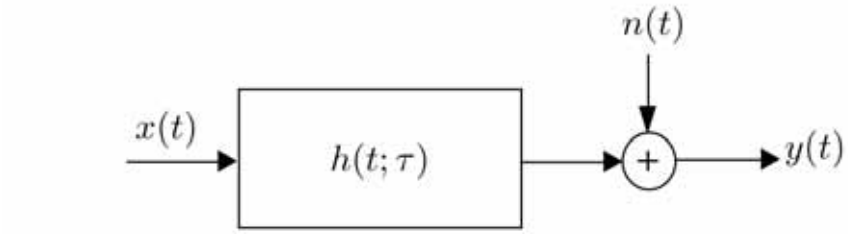

Figure 1.5: Time-varying Single-Input Single-Output(SISO) channel

The Input-Output (I/O) relationship for SISO system can be written as [11]:

$$\begin{aligned} y(t) &= x(t)*h(t;\tau)+n(t) \\ &= \int h(t;\tau)x(t-\tau)d\tau+n(t) \end{aligned} \tag{1.12}$$

Where: $y(t)$ is the system output, $x(t)$ is the system input, $h(t;\tau)$ is the impulse re-

sponse of the channel, and $n(t)$ is the additive white Gaussian noise. For time-selective flat-fading, *non-frequency-selective*, channel the impulse response expressed as:

$$h(t;\tau) = h(t)\delta(\tau) \tag{1.13}$$

Then equation (1.12) becomes:

$$y(t) = h(t)x(t) + n(t) \tag{1.14}$$

For a block of T-symbol length, the output vector $\mathbf{y}$ and input vector $\mathbf{x}$ are described as: $\mathbf{y} = [\ y_1\ y_2\ \cdots\ y_T\ ]$ and $\mathbf{x} = [\ x_1\ x_2\ \cdots\ x_T\ ]$ and the channel gains vector: $\mathbf{h} = [\ h_1\ h_2\ \cdots\ h_T\ ]$. Then, the ergodic capacity of a SISO system can be written as:

$$C_{erg} = E_{\mathbf{h}} log_2(1 + \mathrm{SNR}|\mathbf{h}|^2) \tag{1.15}$$

where $E_{\mathbf{h}}$ is the expected value.

Equation (1.15) defines ergodic capacity, the maximum mutual information averaged over all channel realizations, for SISO system. Outage capacity is defined as the maximum data rate that can be transmitted over the channel with non-zero probability of error. The mathematical definitions for ergodic and outage capacities for MIMO are defined next. Ergodic capacity is used to describe the capacity in fast fading channels. On the other hand, the Outage Capacity is used to characterize the outage probability with any channel rate in slow fading channels [5].

As in the case of SISO system, the input/output relation for MIMO system can be viewed as multi- SISO systems. So, The received signal at i^{th} antenna is denoted by $y_i(t)$ and is expressed as [11]:

$$\begin{aligned} y_i(t) \quad = \quad & \int h_{i1}(t;\tau)x_1(t-\tau)d\tau + \int h_{i2}(t;\tau)x_2(t-\tau)d\tau + \\ & \ldots + \int h_{iN}(t;\tau)x_N(t-\tau)d\tau + n_i(t) \end{aligned} \tag{1.16}$$

$\mathbf{x} : \mathbf{x}(t) = [\ x_1(t)\ x_2(t)\ \cdots\ x_N(t)\ ]^t$represents input vector which includes N transmitted

signals from the BS. The received vector $\mathbf{y} : \mathbf{y}(t) = [\ y_1(t)\ y_2(t)\ \cdots\ y_M(t)\ ]^t$ includes M received signals where $[.]^t$ indicates matrix transpose.

For non-frequency-selective, flat fading channel, the channel impulse response, $h_{ij}(t;\tau) = h_{ij}(t)\delta(\tau)$. So, equation (1.16) can be written as [11]:

$$\begin{aligned} y_i(t) &= h_{i1}(t)x_1(t) + h_{i2}(t)x_2(t) + \\ &\quad \ldots + h_{iN}(t)x_N(t) + n_i(t) \end{aligned} \tag{1.17}$$

where $h_{mn}(t)$is the channel gain between m^{th} receiver element and n^{th} transmitter element. Use matrix notation, the MIMO system based on (1.17) is expressed as:

$$\begin{bmatrix} y_1(t) \\ y_2(t) \\ . \\ . \\ y_N(t) \end{bmatrix} = \begin{bmatrix} h_{11}(t) & h_{12}(t) & .... & h_{1N}(t) \\ h_{21}(t) & h_{22}(t) & .... & h_{2N}(t) \\ . & . & .... & . \\ . & . & .... & . \\ h_{M1}(t) & h_{M2}(t) & .... & h_{MN}(t) \end{bmatrix} \begin{bmatrix} x_1(t) \\ x_2(t) \\ . \\ . \\ x_M(t) \end{bmatrix} + \begin{bmatrix} n_1(t) \\ n_2(t) \\ . \\ . \\ n_M(t) \end{bmatrix} \tag{1.18}$$

Simply, (1.18) can be written as:

$$\mathbf{y}(t) = \mathbf{H}(t)\mathbf{x}(t) + \mathbf{n}(t) \tag{1.19}$$

where $\mathbf{H}(t)$ is the channel gains matrix. and $\mathbf{n} \sim \mathcal{CN}(0, I_N)$, is $N \times 1$ matrix represents the noise term which is assumed to be complex zero-mean Gaussian random process.

For flat-fading MIMO channel, the capacity of the time-varying channel is defined as the sum of capacities of sub-channels averaged over time only. Consider a T-symbol block, the output and input vectors, respectively, are given by [12]:

$$\mathbf{y} = [\ \mathbf{y_1}\ \mathbf{y_2}\ \cdots\ \mathbf{y_T}\ ] \tag{1.20}$$

$$\mathbf{x} = [\ \mathbf{x_1}\ \mathbf{x_2}\ \cdots\ \mathbf{x_T}\ ] \tag{1.21}$$

And the channel matrices can be expressed as:

$$\mathbf{H} = [\ \mathbf{H_1}\ \mathbf{H_2}\ \cdots\ \mathbf{H_T}\ ] \tag{1.22}$$

where $\mathbf{H_i}$ is the channel matrix of block i.

The mutual information between the output and the input can be expressed as [12]:

$$\begin{aligned} I(\mathbf{y};\mathbf{x}) &= I(\mathbf{y};\mathbf{x}|\mathbf{H_1},\mathbf{H_2},...,\mathbf{H_T}) \\ &= \mathrm{E}_{\mathbf{H_1},\mathbf{H_2},...,\mathbf{H_T}}\left[\sum_{k=1}^{T} I(\mathbf{y_k};\mathbf{x_k}|\mathbf{H_k})\right] \\ &= \mathrm{E}_{\mathbf{H_1},\mathbf{H_2},...,\mathbf{H_T}}\sum_{k=1}^{T}\left[log\left(det\left(I+Q\mathbf{H_k}{\mathbf{H_k}}^{\mathcal{H}}\right)\right)\right] \\ &= T\mathrm{E}_{\mathbf{H}}\left[log\left(det\left(I+Q\mathbf{H}\mathbf{H}^{\mathcal{H}}\right)\right)\right] \end{aligned} \tag{1.23}$$

where $[.]^{\mathcal{H}}$ means transpose conjugation operation and $\mathbf{Q}$ is the input covariance matrix. The ergodic capacity for time-varying MIMO channel is obtained by taking time average of (1.23) as [13]:

$$\mathrm{C}_{erg} = E_{\mathbf{H}}\left\{\log\left(\det\left(I+Q\mathbf{H}\mathbf{H}^{\mathcal{H}}\right)\right)\right\} \tag{1.24}$$

where $\mathbf{Q} = \frac{P}{N}\mathbf{I}_N$ in case of uniform power allocation scheme and P is the total transmitted power.

In case of outage capacity, the transmission rate is fixed; say R and the data will not be correctly received if R is greater than the capacity supported by the channel. The outage probability is defined as the probability of incorrect reception [14] and is defined as:

$$\mathcal{P}_{out} = \mathcal{P}\left(\log\left(det\left(I+Q\mathbf{H}\mathbf{H}^{\mathcal{H}}\right)\right) < R\right) \tag{1.25}$$

In general, it is hard to find the capacity for time-varying frequency-selective fading channel. So, the capacity is approximated by dividing up the channel bandwidth(B) into sub-channels with coherence bandwidth and assume the resulting sub-channels are independent, time-varying, and flat-fading channels [13]. Then, the total capacity is the sum of capacities of sub-channels subject to the power constraint averaged over both time and

frequency [13]. Obviously, the capacity of a MIMO channel depends on :

1. The channel averaged SNR .
2. Channel Knowledge,what is known about the channel information at transmitter and receiver sides.
3. The correlation between channel gains on each antenna.

1.4 CHANNEL SIDE INFORMATION

We note that for a time-varying MIMO channel there are different definitions for the capacity which mainly depends on the availability of channel state information or channel distribution at the transmitter and/or the receiver. channel side information can be classified into three main groups as [5]:

Group 1. Perfect Channel State Information at Receiver (CSIR) and perfect Channel State Information at the Transmitter (CSIT). In this case, the transmitter and receiver have instantaneous knowledge about the channel and the transmitter can adapt its transmission strategy (power/rate). Perfect CSIT can be achieved by a feedback link to the transmitter. However, this link may be impaired by noise and due delay which result in degradation of the overall performance of the system.

Group 2. Perfect CSIR and perfect Channel Distribution Information at the Transmitter (CDIT). In this case, the receiver keeps tracking the channel state while transmitter has only information about the distribution of the channel. channel statistics change due the to mobility of environment, the transmitter, the receiver. statistical properties depend on the time interval in which statistics are fed back to the transmitter. in other word, for short-time interval the channel realizations, $\mathbf{H}$, may have non-zero mean and certain correlation between entries that reflect the channel environment. in contrast, for long-time interval the channel matrix, $\mathbf{H}$, may have zero-mean with uncorrelated entries [5, 15] due to averaging over many propagation environments .

Group 3. Channel Distribution Information at the Receiver (CDIR) and CDIT. In this case, the transmitter and receiver have only information about the distribution of the channel.

Group 4. Quantized Channel State Information: In this group, the CSI is assumed to be perfectly known at the receiver. The Receiver feeds $N_B - bit$ quantization of the channel information to the transmitter. It is applicable for slow fading scenarios, where the receiver feeds back quantized information about the channel at the beginning of each block. There are three special models for the distribution of the channel [5]:

(a) Zero-Mean Spatially White (ZMSW) model.

(b) Channel Mean Information (CMI) model.

(c) Channel Covariance Information (CCI) model.

In the three channel models, the channel is modeled as complex Gaussian random variables. The ZMSW model is the most common model for the channel distribution where the channel gains are modeled as Independent and identically distributed (i.i.d), zero-mean, unit variance, complex circularly symmetric Gaussian random variables. Therefore, $\mathbf{H}$ is written as [5]:

$$\mathbf{H} \sim \mathcal{CN}(\mathbf{0}, \mathbf{I}) \tag{1.26}$$

The CMI model is referred to as Mean feedback model where the channel distribution has non-zero mean and white covariance matrix. In this case, the distribution of the channel is described as [5]:

$$\mathbf{H} \sim \mathcal{CN}\left(\mathrm{E}\{\mathbf{H}\}, \sigma^2\mathbf{I}\right) \tag{1.27}$$

In the CCI model, which also known as covariance feedback model, the channel distribution is described as [5]:

$$\mathbf{H} \sim \mathcal{CN}(\mathbf{0}, \Sigma_H) \tag{1.28}$$

العنوان:	-Realistic Modeling of Time-Varying MIMO Channel Capacity Using Ray Tracing in Multi-Ring Scattering Environment
المؤلف الرئيسي:	Shtaiwi, Eyad Mahmoud
مؤلفين آخرين:	Harb, Bassam(Advisor)
التاريخ الميلادي:	2015
موقع:	إربد
الصفحات:	1 - 64
رقم MD:	747732
نوع المحتوى:	رسائل جامعية
اللغة:	English
الدرجة العلمية:	رسالة ماجستير
الجامعة:	جامعة اليرموك
الكلية:	كلية الحجاوي للهندسة التكنولوجية
الدولة:	الاردن
قواعد المعلومات:	Dissertations
مواضيع:	أنظمة الاتصالات اللاسلكية
رابط:	https://search.mandumah.com/Record/747732

Chapter 4

ANALYSIS AND SIMULATION

4.1 ANALYSIS METHODS

In this thesis, we evaluate the capacity of a time-varying MIMO channel in two ways, see Figure 4.2 :

- **FIRST**: Using RT Simulator

  We followed the following steps to compute the capacity of the MIMO channel:

  (a) The geometry and location of local scattering are required as input to RT-Simulator. We have an information for a city and we used it to run our simulator. The location for the base-station is fixed and the moving mobile station locations are randomly selected, points are also dependent of speed. We developed a MATLAB code to illustrate the bulding in 3D. Figure 4.2 shows top view of the buildings used in the RT-simulator.

  (b) The information regarding the operating frequency, Antenna separations, and order of reflections are other parameters needed to run RT-Simulator. Figure5.2 represents setup of input parameters for RT-Simulator.

  (c) Outputs of the RT are: Received electrical field as expressed in Eq.(3.9), Time-of-Arrival (ToA) information, and phases of each ray as well as the total num-

Table 4.1: Ray Tracing Simulator Parameters value

Parameter	Value
Operating frequency(f_o)	3.6GHz
Length of Dipole	$\frac{\lambda}{2}$
Dipole current	1.0 A
Propagation factor	$2\pi\sqrt{\mu_0\varepsilon_0}f_o$

ber of rays received at MS.

(d) Equation(3.10) used to find channel gains, based on the outputs of RT.

(e) Based on the computed channel gains, the channel matrix realizations, H, are constructed.

(f) Using the channel matrix realization, H, the channel capacity is computed as:

$$\mathrm{C} = \log\left(\det\left(I + \frac{SNR}{N}HH^{\mathcal{H}}\right)\right) \tag{4.1}$$

(g) Changing the locations for both MS and BS and repeat steps (a)-(f) 10000 times .

(h) Compute the capacity by averaging the capacities in previous steps as:

$$\mathrm{C}_{erg} = \frac{\sum_{i=1}^{10000} C}{10000} \tag{4.2}$$

- **SECOND**: Theoretically based on space-time covariance model

  In this approach, We compute the capacity of time-varying MIMO channel when there is neither CSIT nor CSIR. The distribution of the channel follows CCI model considering the motion effect and the correlation between channels resulting from antenna's separation. since ZMSW requires conditions which are not always happened. CMI model is not valid in highly mobile channel.

  We compute the capacity based on the estimated channel distribution in any scattering environment, especially in multi-ring environments. The Capacity is computed as follow:

Figure 4.1: Top view of the city's buildings used in RT-Simulator

(a) Assume channel distribution **H** modeled as:

$$\mathbf{H} \sim \mathcal{CN}(\mathbf{0}, \Sigma_H) \tag{4.3}$$

Since the covariance matrix gives critical information for understanding the performance of the system. As well as, the complex channel gains computed from the data collected from RT are used to estimate the best distribution that fits the channel. We found that the histograms of real and imaginary parts of the channel gains are close to Gaussian distribution with zero mean but not unity covariance, see Figure 4.3.

(b) The entries of estimated covariance matrix of time-vary MIMO channel is computed using (3.4):

$$\mathrm{E}\left\{h_{p,r}(t)h^{*}_{q,s}(t+\Delta t)\right\} = \mathrm{E}\left\{\sum_{m=0}^{K-1} A_m^2 \; e^{j2\pi f_d \Delta t \cos\alpha_m} e^{j\frac{2\pi d_{rs}}{\lambda}\cos(\phi_m-\gamma_{rs})} \; e^{j\frac{2\pi D_{pq}}{\lambda}\cos(\theta_m-\Gamma_{pq})}\right\} \tag{4.4}$$

To compute (4.4) we need the PDF of joint AOA and AoD which is given in (3.8) as:

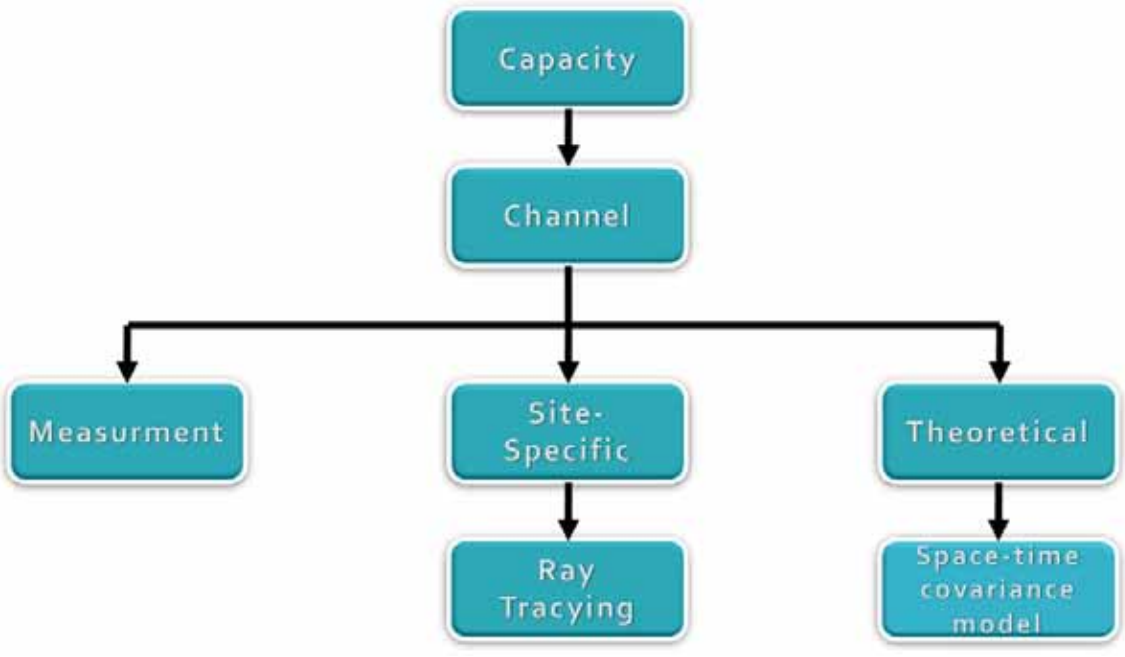

Figure 4.2: Flowchart of analysis and simulation methods

$$p^{(k)}_{\phi,\theta}(\phi,\theta) = \begin{cases} D^{k+1}\frac{(k+1)}{2\pi R^{k+1}}\frac{|\sin(\theta)|\sin^k(\phi)}{\sin^{k+2}(\theta-\phi)} & , (\phi,\theta)\in\mathcal{R} \\ 0 & , \text{otherwise} \end{cases} \tag{4.5}$$

$$\mathcal{R} \in \left\{(\phi,\theta) \mid 0 \le \frac{D\sin(\phi)}{\sin(\theta-\phi)} \le R, \theta \ne \phi\right\}$$

So,

$$\mathrm{E}\left\{h_{p,r}(t)h^*_{q,s}(t+\Delta t)\right\} = \mathrm{E}\left\{\sum_{m=0}^{K-1} A_m^2\, e^{j2\pi f_d \Delta t\cos\alpha_m} e^{j\frac{2\pi d_{rs}}{\lambda}\cos(\phi_m-\gamma_{rs})}\, e^{j\frac{2\pi D_{pq}}{\lambda}\cos(\theta_m-\Gamma_{pq})}\right\}$$

$$= \int_{\theta=-\pi}^{\pi}\int_{\phi=-\phi_0}^{\phi_0} \left(\frac{D}{R}\right)^{k+1}\frac{(k+1)}{2\pi}\frac{|\sin(\theta)|\sin^k(\phi)}{\sin^{k+2}(\theta-\phi)} e^{j2\pi f_d\Delta t\cos\alpha_m} e^{j\frac{2\pi d_{rs}}{\lambda}\cos(\phi-\gamma)} e^{j\frac{2\pi D_{pq}}{\lambda}\cos(\theta-\Gamma)} d\phi d\theta \tag{4.6}$$

Where : $\phi_0 = \arcsin(\frac{R}{D})$.

We note that the covariance matrix is function of Doppler spread, Scattering distribution and density, propagation environment, and antenna configurations

and separations.

(c) After computing the covariance matrix of the channel. We compute the capacity using Monte-Carlo simulation as:

– We generate matrix channel realizations for 1000 times:

$$H = \Sigma_H^{1/2} H_{iid} \tag{4.7}$$

Where: $H_{iid} \sim \mathcal{CN}(0, \mathbf{I})$

– We compute the capacity of the channel for each channel realiztion, H, as:

$$\mathrm{C} = \left\{ \log \left(\det \left(I + \frac{SNR}{N} H H^{\mathcal{H}} \right) \right) \right\} \tag{4.8}$$

– The Ergodic capacity is the average of the capacities of each channel realization:

$$\mathrm{C}_{erg} = \frac{\Sigma_{i=1}^{1000} C}{1000} \tag{4.9}$$

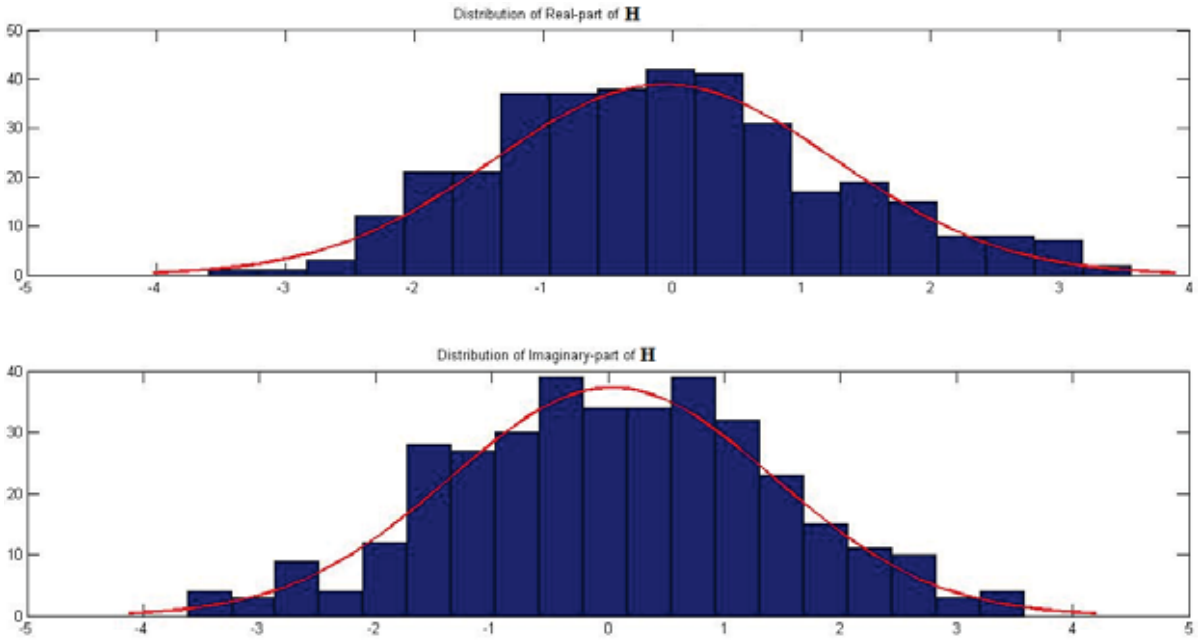

Figure 4.3: Histogram of channel gains - Ray-Tracer(RT)

4.2 SIMULATION RESULTS

In this section, we present results for computed capacity for time-varying MIMO channel using RT-simulator and mathematical calculations based on the proposed model for scattering geometry. Table 4.1 shows the covariance matrix for time-varying MIMO channel for different scenarios which computed by the integral in (Eq.4.6). The integral is computed numerical using Mupad toolbox in MATLAB. We assume that $R/D = 0.125$. δ_D represents antenna separation at BS, and δ_d is the antenna separation at MS. k is the shape factor which controls the density and distribution local scattering. However, Table 4.2 shows the covariance matrix for measured time-varying MIMO channel for two cases when the local scattering are moderate and rich. [23, 65]:

Table 4.2: Measured Covariance Matrix

Σ_H	**Model**
$\begin{bmatrix} 0.95 & 0.39 & 0.071-j0.93 & 0.024-j0.17 \\ 0.39 & 1.03 & 0.028-j0.18 & 0.076-j0.43 \\ 0.071+j0.39 & 0.028-j0.18 & 0.97 & 0.042+j0.0025 \\ 0.024+j0.17 & 0.076-j0.43 & 0.042+j0.0025 & 1.05 \end{bmatrix}$	Moderate Scattering
$\begin{bmatrix} 1.04 & -0.0096-j0.059 & -0.3-j0.32 & 0.0091+j0.013 \\ -0.0096+j0.059 & 0.97 & 0.039+j0.029 & -0.29-j0.28 \\ -0.3+j0.32 & 0.039-j0.029 & 1.02 & 0.0082-j0.079 \\ 0.0091-j0.013 & -0.29+j0.28 & 0.0082+j0.079 & 0.97 \end{bmatrix}$	Rich scattering

Figure 4.4 shows the results for time-varying MIMO channel capacity which are computed by two methods described in the proposed approach. Where the mean (ergodic) capacity for MIMO channels for each case in Tables 4.1 and 4.2 and measured channel by RT simulator are plotted. Figure 4.5- Figure 4.8 depict difference percentage of ergodic capacities compared to i.i.d channels.

We clearly recognize that the performance of measured MIMO channels wouldn't be as theoretical performance of the channel even though the measurements are conducted

in a rich scattering environments. We also note that the poor performance achieved when the scattering environment looks a Gaussian-like. This makes sense since the scatterers are located close to MS block the signal from reaching MS.

We Note that in some cases the error percentage between the ideal model and the estimated capacity is greater than 90%, see Figure 4.4 . Where the error between measured and i.i.d channel is $= 30\%$. The difference in low SNR-regime is much greater than the difference in high SNR-regime.

Simulation results show that the classical channel model; i.i.d Rayleigh fading, is not always correctly describe time-varying MIMO channel see Figure 4.3 . In addition, we clear the idea that the amount of correlation between channels is dependent of antenna separation, distribution and density of local scatterers. Taking the case where $k = 25$, we investigate the capacity for time-varying MIMO channel for the case in See Figure 4.3 . We note that for sufficient separations where antennas' elements at both the BS and MS are spaced, $\delta_D = 11\lambda$ and $\delta_d = 0.38\lambda$, in addition to large number of scatterers, the covariance matrix $\Sigma_H \approx \mathbf{I}$. and mean capacity is almost matches that for i.i.d channel. In contrast, for the same scattering distribution and density, $k = 25$, we see how antenna separations, ,$\delta_D = 3\lambda$ and $\delta_d = 0.5\lambda$, increase the correlation between channel gains and how that is reflected on the performance of the system. As well, we explore the effect of Doppler spread, f_d, of the capacity of the channel. We spaced antennas' elements in way that reduce the correlation between every (Tx-Rx) link, $\delta_D = 11\lambda$ and $\delta_d = 0.38\lambda$. Then we computed the capacity by considering the effect of Doppler spread. we note the degradation of the capacity for moving MS. We assume that the normalized Doppler frequency $f_d \Delta t = 0.1$.

Table 4.3: Computed Covariance Matrix

Σ_H	δ_D/λ	δ_d/λ	k	$f_d\Delta t$
$\begin{bmatrix} 1 & 0.0176+j0.0023 & 0.0062+j0.0004 & 0.0302+j0.0326 \\ 0.0176-j0.0023 & 1 & 0.006184-j0.0004 & 0.0062+j0.0004 \\ 0.0062-j0.0004 & 0.006184+j0.0004 & 1 & 0.0176+j0.0023 \\ 0.0302-j0.0326 & 0.0062-j0.0004 & 0.0176-j0.0023 & 1 \end{bmatrix}$	3.8	0.35	10	0
$\begin{bmatrix} 1 & -0.0036 & -0.0041-j0.0006 & -0.006-j0.002 \\ -0.0036 & 1 & -0.0050-j0.0008 & -0.0041-j0.0006 \\ -0.0041+j0.0006 & -0.0050+j0.0008 & 1 & -0.0036 \\ -0.006+j0.002 & -0.0041+j0.0006 & -0.0036 & 1 \end{bmatrix}$	11	0.38	25	0
$\begin{bmatrix} 1 & -0.0158-j0.0312 & -0.017-j0.0032 & -0.0026 \\ -0.0158+j0.0312 & 1 & -0.0026 & -0.017-j0.0032 \\ -0.017+j0.0032 & -0.0026 & 1 & -0.0158-j0.0312 \\ -0.0026 & -0.017+j0.0032 & -0.0158+j0.0312 & 1 \end{bmatrix}$	3	0.5	25	0
$\begin{bmatrix} 1 & 0.0197+j0.1098 & 0.2829+j0.0394 & -0.002+j0.1101 \\ 0.0197-j0.1098 & 1 & 0.0321-j0.1098 & 0.2829+j0.0394 \\ 0.2829-j0.0394 & 0.0321+j0.1098 & 1 & 0.0197+j0.1098 \\ -0.002-j0.1101 & 0.2829-j0.0394 & 0.0197-j0.1098 & 1 \end{bmatrix}$	0.5	0.5	0	0
$\begin{bmatrix} 1 & -0.0212+j0.0002 & -0.0032-j0.0004 & -0.004-j0.001 \\ -0.0212-j0.0002 & 1 & -0.006-j0.001 & -0.0032-j0.0004 \\ -0.0032+j0.0004 & -0.006+j0.001 & 1 & -0.0212+j0.0002 \\ -0.004+j0.001 & -0.0032+j0.0004 & -0.0212-j0.0002 & 1 \end{bmatrix}$	11	0.5	25	0.1

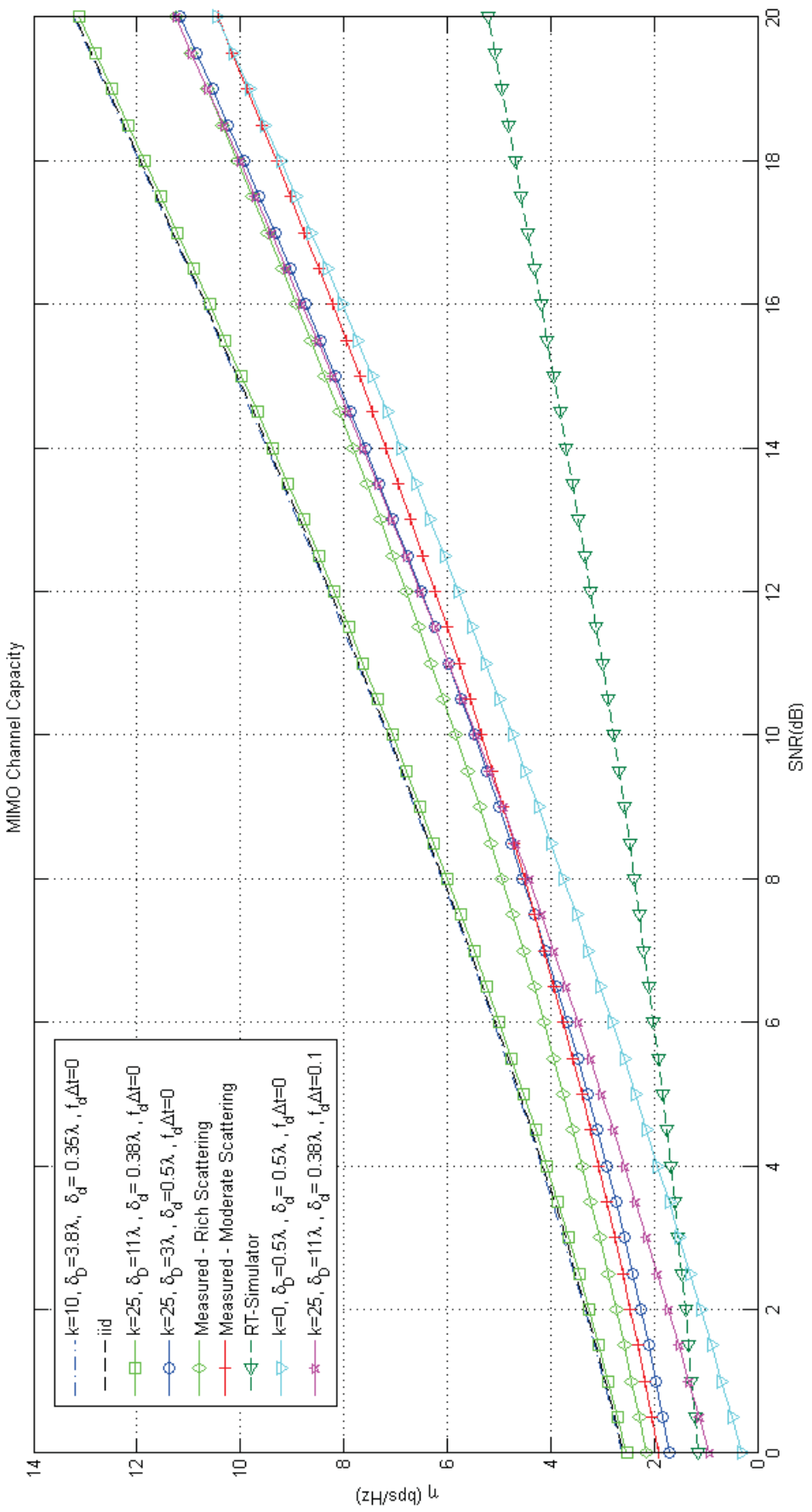

Figure 4.4: Capacities (ergodic) for MIMO channels in Table6.1 and Table6.2

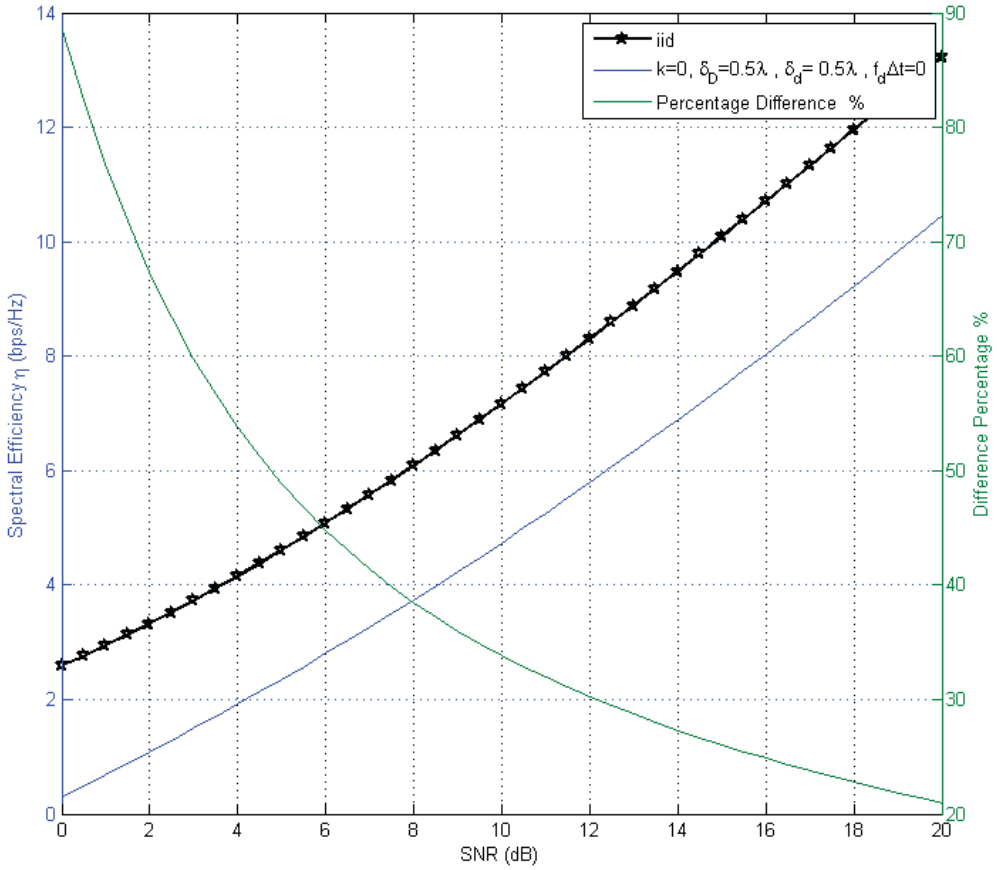

Figure 4.5: Comparison between ergodic capacities when $k = 0$ and iid channel

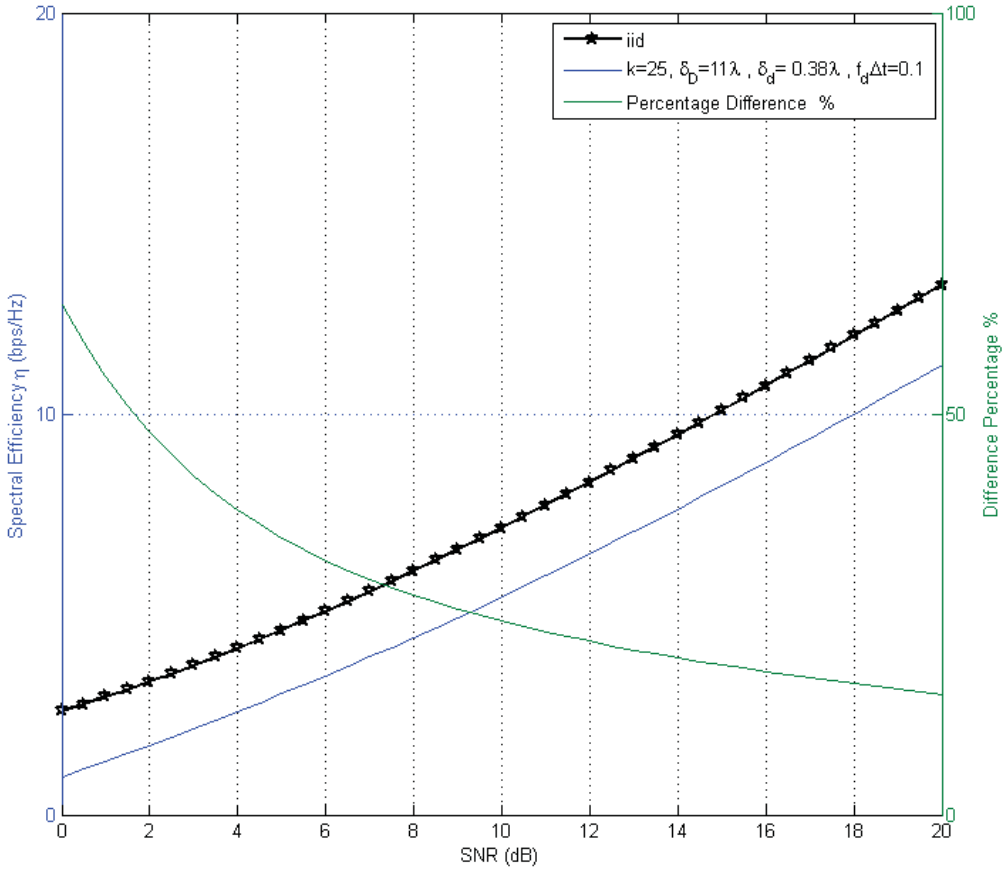

Figure 4.6: Ergodic capacity comparison when $k = 25$, $\delta_D = 11\lambda$, $\delta_d = 0.38\lambda$, $f_d\Delta t = 0.1$ *and iid channel*

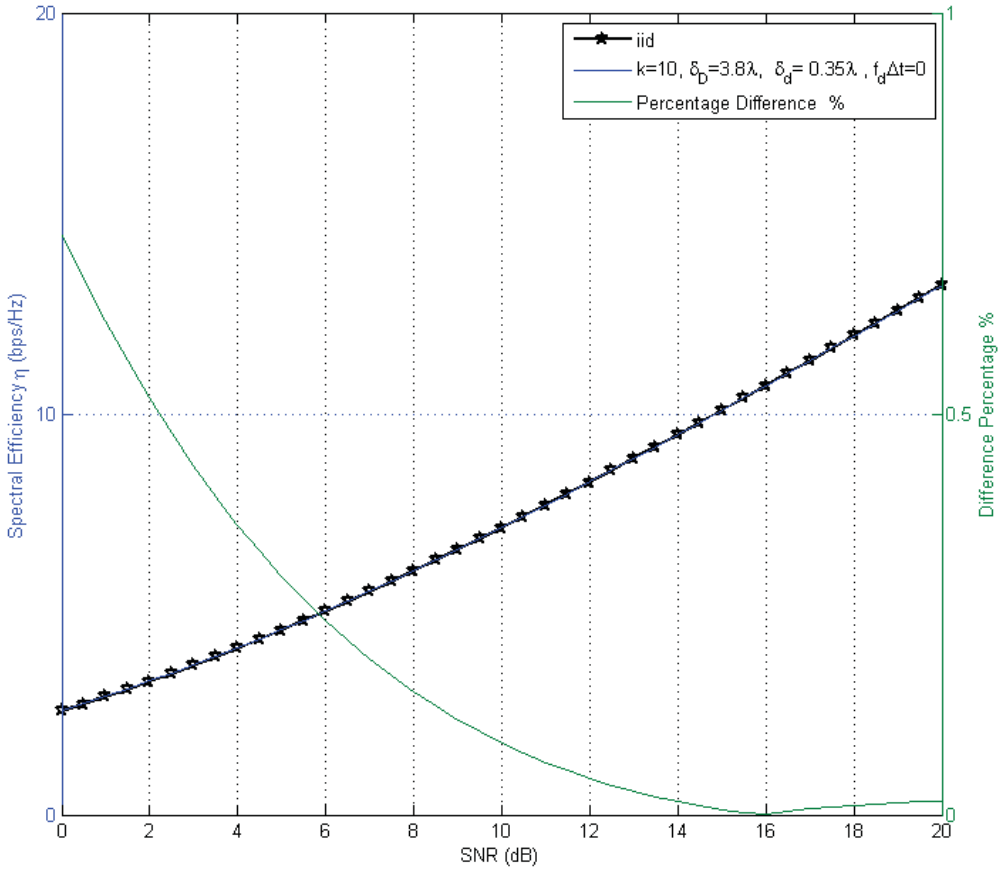

Figure 4.7: Ergodic capacity comparison when $k = 10$, $\delta_D = 3.8\lambda$, $\delta_d = 0.35\lambda$, $f_d \Delta t = 0$ *and iid channel*

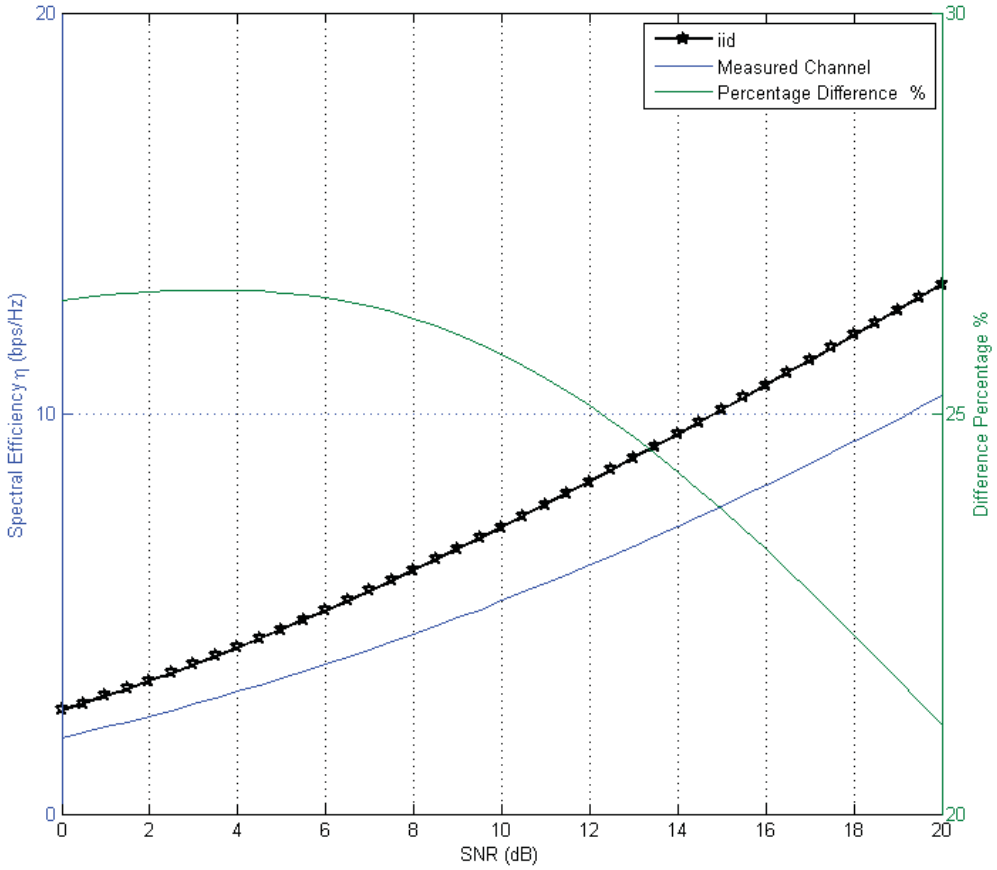

Figure 4.8: Ergodic capacity comparison between measured and iid channels

Chapter 5

CONCLUSIONS AND FUTURE WORK

In this thesis, we have computed ergodic capacity of time-varying MIMO channel using space-time covariance model and RT-simulator. Many searches show that the classical independent and identically distributed Rayleigh fading channel is not always fit real scenarios. So, the need for a realistic model for the channel is arise. We present a model for time-varying MIMO channel which is applicable for arbitrary scattering distribution and density.

In summary, We evaluate the capacity of a time-varying MIMO channel by three methods; theoretically, site-specific technique and measurements. the computed capacity is compared with the measured capacity and we note the following:

- The classical (i.i.d) Rayleigh fading channel is not always valid even we guarantee a rich scattering environment. It is required a sufficient antenna elements separations.
- Amount of correlation depends on scattering distribution and spacing between antenna's elements.
- Doppler spread effect should be considered in the design of any wireless communication system. Since we note the degradation in the performance of the MIMO channel due to Doppler spread.

5.1 FUTURE WORK

As a future work, we can consider the following:

- The effect of local scatterers around base-station (BS)can be used to evaluate the performance of MIMO system in case of peer-to-peer transmission.
- More complex array configuration can be considered rather than uniform linear array (ULA).
- We can extend this model to deal with multi-user MIMO wireless networks since single-user case used to channalized wireless systems.

العنوان:	-Realistic Modeling of Time-Varying MIMO Channel Capacity Using Ray Tracing in Multi-Ring Scattering Environment
المؤلف الرئيسي:	Shtaiwi, Eyad Mahmoud
مؤلفين آخرين:	Harb, Bassam(Advisor)
التاريخ الميلادي:	2015
موقع:	إربد
الصفحات:	1 - 64
رقم MD:	747732
نوع المحتوى:	رسائل جامعية
اللغة:	English
الدرجة العلمية:	رسالة ماجستير
الجامعة:	جامعة اليرموك
الكلية:	كلية الحجاوي للهندسة التكنولوجية
الدولة:	الاردن
قواعد المعلومات:	Dissertations
مواضيع:	أنظمة الاتصالات اللاسلكية
رابط:	https://search.mandumah.com/Record/747732

References

[1] D. Gesbert, M. Shafi, D.-s. Shiu, P. J. Smith, and A. Naguib, "From theory to practice: an overview of mimo space-time coded wireless systems," *Selected Areas in Communications, IEEE Journal on*, vol. 21, no. 3, pp. 281–302, 2003.

[2] A. Paulraj, D. GORE, R. Nabar, and H. Bolcskei, "An overview of mimo communications - a key to gigabit wireless," *Proceedings of the IEEE*, vol. 92, pp. 198–218, Feb 2004.

[3] D. Tse and P. Viswanath, *Fundamentals of wireless communication*. Cambridge University Press, 2005.

[4] J. Mietzner, R. Schober, L. Lampe, W. H. Gerstacker, and P. A. Hoeher, "Multiple-antenna techniques for wireless communications-a comprehensive literature survey," *Communications Surveys & Tutorials, IEEE*, vol. 11, no. 2, pp. 87–105, 2009.

[5] E. Biglieri, R. Calderbank, A. Constantinides, A. Goldsmith, A. Paulraj, and H. V. Poor, *MIMO wireless communications*. Cambridge University Press, 2007.

[6] N. Boubaker, K. Letaief, and D. Ross, "Performance of blast over frequency-selective wireless communication channels," *Communications, IEEE Transactions on*, vol. 50, pp. 196–199, Feb 2002.

[7] A. Lozano and C. Papadias, "Layered space-time receivers for frequency-selective wireless channels," *Communications, IEEE Transactions on*, vol. 50, pp. 65–73, Jan 2002.

[8] M. Chiani, M. Win, and A. Zanella, "On the capacity of spatially correlated mimo rayleigh-fading channels," *Information Theory, IEEE Transactions on*, vol. 49, pp. 2363–2371, Oct 2003.

[9] C. Shannon, "Communication in the presence of noise," *Proceedings of the IRE*, vol. 37, pp. 10–21, Jan 1949.

[10] C. Shannon, "A mathematical theory of communication," *Bell System Technical Journal, The*, vol. 27, pp. 379–423, July 1948.

[11] E. Biglieri, *Coding for wireless channels*. Springer Science & Business Media, 2005.

[12] Y. Liang and V. Veeravalli, "Capacity of noncoherent time-selective block rayleigh flat-fading channel," in *Information Theory, 2002. Proceedings. 2002 IEEE International Symposium on*, p. 166, IEEE, 2002.

[13] A. Goldsmith, *Wireless communications*. Cambridge university press, 2005.

[14] E. Telatar, "Capacity of multi-antenna gaussian channels," *European transactions on telecommunications*, vol. 10, no. 6, pp. 585–595, 1999.

[15] S. Jafar, S. Vishwanath, and A. Goldsmith, "Channel capacity and beamforming for multiple transmit and receive antennas with covariance feedback," in *Communications, 2001. ICC 2001. IEEE International Conference on*, vol. 7, pp. 2266–2270 vol.7, 2001.

[16] I. Viering, H. Hofstetter, and W. Utschick, "Validity of spatial covariance matrices over time and frequency," in *Global Telecommunications Conference, 2002. GLOBECOM '02. IEEE*, vol. 1, pp. 851–855 vol.1, Nov 2002.

[17] C.-N. Chuah, D. Tse, J. Kahn, and R. Valenzuela, "Capacity scaling in mimo wireless systems under correlated fading," *Information Theory, IEEE Transactions on*, vol. 48, pp. 637–650, Mar 2002.

[18] W. Chao, W. Shunjun, Z. Linrang, and T. Xiaoyan, "Capacity evaluation of mimo systems by monte-carlo methods," in *Neural Networks and Signal Processing, 2003. Proceedings of the 2003 International Conference on*, vol. 2, pp. 1464–1466 Vol.2, Dec 2003.

[19] R. Perera, T. Pollock, and T. Abhayapala, "Upper bound on non-coherent mimo channel capacity in rayleigh fading," in *Communications, 2005 Asia-Pacific Conference on*, pp. 72–76, Oct 2005.

[20] M.-A. Khalighi, J. Brossier, G. Jourdain, and K. Raoof, "Water filling capacity of rayleigh mimo channels," in *Personal, Indoor and Mobile Radio Communications, 2001 12th IEEE International Symposium on*, vol. 1, pp. A–155–A–158 vol.1, Sep 2001.

[21] R. Vieira, J. Brandao, and G. Siqueira, "Mimo measured channels: Capacity results and analysis of channel parameters," in *Telecommunications Symposium, 2006 International*, pp. 152–157, Sept 2006.

[22] T. Kan, R. Funada, J. Wang, H. Harada, and J.-i. Takada, "Mimo channel capacity of a measured radio channel for outdoor macro cellular systems at 3ghz-band," in *Vehicular Technology Conference Fall (VTC 2009-Fall), 2009 IEEE 70th*, pp. 1–5, Sept 2009.

[23] A. Molisch, M. Steinbauer, M. Toeltsch, E. Bonek, and R. Thoma, "Capacity of mimo systems based on measured wireless channels," *Selected Areas in Communications, IEEE Journal on*, vol. 20, pp. 561–569, Apr 2002.

[24] S. Jayaweera and H. Poor, "Capacity of multiple-antenna systems with both receiver and transmitter channel state information," *Information Theory, IEEE Transactions on*, vol. 49, pp. 2697–2709, Oct 2003.

[25] J. C. Roh and B. Rao, "An efficient feedback method for mimo systems with slowly time-varying channels," in *Wireless Communications and Networking Conference, 2004. WCNC. 2004 IEEE*, vol. 2, pp. 760–764 Vol.2, March 2004.

[26] M. Sadrabadi, M. A. Maddah-Ali, and A. K. Khandani, "On the capacity of time-varying channels with periodic feedback," *Information Theory, IEEE Transactions on*, vol. 53, pp. 2910–2915, Aug 2007.

[27] E. Visotsky and U. Madhow, "Space-time transmit precoding with imperfect feedback," *Information Theory, IEEE Transactions on*, vol. 47, pp. 2632–2639, Sep 2001.

[28] E. Jorswieck and H. Boche, "Channel capacity and capacity-range of beamforming in mimo wireless systems under correlated fading with covariance feedback," *Wireless Communications, IEEE Transactions on*, vol. 3, pp. 1543–1553, Sept 2004.

[29] S. Jafar and A. Goldsmith, "On optimality of beamforming for multiple antenna systems with imperfect feedback," in *Information Theory, 2001. Proceedings. 2001 IEEE International Symposium on*, pp. 321–, 2001.

[30] K. Kobayashi, T. Ohtsuki, and T. Kaneko, "Mimo systems in the presence of feedback delay," in *Communications, 2006. ICC '06. IEEE International Conference on*, vol. 9, pp. 4102–4106, June 2006.

[31] W. Zhou, C. Kai, and X. Li, "Mimo system capacity with imperfect feedback channel," in *Communications and Networking in China (CHINACOM), 2012 7th International ICST Conference on*, pp. 399–402, Aug 2012.

[32] S. Banani and R. Vaughan, "The effect of training-based channel estimation on the capacity of closed-loop mimo systems with imperfect csi feedback," in *Vehicular Technology Conference Fall (VTC 2010-Fall), 2010 IEEE 72nd*, pp. 1–5, Sept 2010.

[33] A. Mukherjee and H. Kwon, "Enhanced svd-based transmit pre-processing for single-user and multi-user mimo wireless systems with imperfect csit," in *Signals, Systems and Computers, 2007. ACSSC 2007. Conference Record of the Forty-First Asilomar Conference on*, pp. 1659–1663, Nov 2007.

[34] G. Lebrun, J. Gao, and M. Faulkner, "Mimo transmission over a time-varying channel using svd," *Wireless Communications, IEEE Transactions on*, vol. 4, pp. 757–764, March 2005.

[35] D. Tse, C.-N. Chuah, and J. Kahn, "Capacity scaling in dual-antenna-array wireless systems," in *Wireless Communications and Networking Confernce, 2000. WCNC. 2000 IEEE*, vol. 1, pp. 25–29 vol.1, 2000.

[36] M. Kamath and B. Hughes, "The asymptotic capacity of multiple-antenna rayleigh-fading channels," *Information Theory, IEEE Transactions on*, vol. 51, pp. 4325–4333, Dec 2005.

[37] X. Lv, K. Liu, and Y. Ma, "Some results on the capacity of mimo rayleigh fading channels," in *Wireless Communications Networking and Mobile Computing (WiCOM), 2010 6th International Conference on*, pp. 1–4, Sept 2010.

[38] G. Foschini and M. Gans, "On limits of wireless communications in a fading environment when using multiple antennas," *Wireless Personal Communications*, vol. 6, no. 3, pp. 311–335, 1998.

[39] A. Goldsmith, S. Jafar, N. Jindal, and S. Vishwanath, "Capacity limits of mimo channels," *Selected Areas in Communications, IEEE Journal on*, vol. 21, pp. 684–702, June 2003.

[40] A. Goldsmith, S. Jafar, N. Jindal, and S. Vishwanath, "Capacity limits of mimo channels," *Selected Areas in Communications, IEEE Journal on*, vol. 21, pp. 684–702, June 2003.

[41] V. Raghavan, A. Sayeed, and J. H. Kotecha, "Impact of mismatched statistics on correlated mimo capacity," in *Acoustics, Speech and Signal Processing, 2008. ICASSP 2008. IEEE International Conference on*, pp. 3025–3028, March 2008.

[42] O. Oyman, R. Nabar, H. Bolcskei, and A. Paulraj, "Characterizing the statistical properties of mutual information in mimo channels," *Signal Processing, IEEE Transactions on*, vol. 51, pp. 2784–2795, Nov 2003.

[43] P. Smith and M. Shafi, "An approximate capacity distribution for mimo systems," *Communications, IEEE Transactions on*, vol. 52, pp. 887–890, June 2004.

[44] H. ping ZHANG, P. WU, and A. jun LIU, "Ergodic channel capacity of the spatial correlated rayleigh {MIMO} channel," *The Journal of China Universities of Posts and Telecommunications*, vol. 14, no. 4, pp. 32 – 35, 2007.

[45] C. Oestges, B. Clerckx, D. Vanhoenacker-Janvier, and A. Paulraj, "Impact of diagonal correlations on mimo capacity: application to geometrical scattering models," in *Vehicular Technology Conference, 2003. VTC 2003-Fall. 2003 IEEE 58th*, vol. 1, pp. 394–398 Vol.1, Oct 2003.

[46] L. Wood and W. Hodgkiss, "Mimo channel models and performance metrics," in *Global Telecommunications Conference, 2007. GLOBECOM '07. IEEE*, pp. 3740–3744, Nov 2007.

[47] H. Ozcelik, N. Czink, and E. Bonek, "What makes a good mimo channel model?," in *Vehicular Technology Conference, 2005. VTC 2005-Spring. 2005 IEEE 61st*, vol. 1, pp. 156–160 Vol. 1, May 2005.

[48] A. Maaref and S. Aissa, "Impact of spatial fading correlation and keyholes on the capacity of mimo systems with transmitter and receiver csi," in *Communications, 2007. ICC '07. IEEE International Conference on*, pp. 4357–4362, June 2007.

[49] H. Ozcelik, M. Herdin, W. Weichselberger, J. Wallace, and E. Bonek, "Deficiencies of 'kronecker' mimo radio channel model," *Electronics Letters*, vol. 39, pp. 1209–1210, Aug 2003.

[50] C. Oestges, "Validity of the kronecker model for mimo correlated channels," in *Vehicular Technology Conference, 2006. VTC 2006-Spring. IEEE 63rd*, vol. 6, pp. 2818–2822, May 2006.

[51] W. C. Jakes, *Microwave Mobile Communications*. May 1974.

[52] R. Clarke, "A statistical theory of mobile-radio reception," *Bell System Technical Journal, The*, vol. 47, pp. 957–1000, July 1968.

[53] T.-A. Chen, M. Fitz, W.-Y. Kuo, M. Zoltowski, and J. Grimm, "A space-time model for frequency nonselective rayleigh fading channels with applications to space-time modems," *Selected Areas in Communications, IEEE Journal on*, vol. 18, pp. 1175–1190, July 2000.

[54] R. G. Gallager, "Circularly-symmetric gaussian random vectors," pp. 1–9, Jan 2008.

[55] D. shan Shiu, G. Faschini, M. Gans, and J. Kahn, "Fading correlation and its effect on the capacity of multi-element antenna systems," in *Universal Personal Communications, 1998. ICUPC '98. IEEE 1998 International Conference on*, vol. 1, pp. 429–433 vol.1, Oct 1998.

[56] L. T. Younkins, "on the performance of multi antenna techniques for spatially and temporally correlated wireless channels."

[57] Y. Yang and M. Jensen, "Mimo channel spatial covariance estimation: Analysis using a closed-form model," in *Wireless Information Technology and Systems (ICWITS), 2010 IEEE International Conference on*, pp. 1–4, Aug 2010.

[58] A. Borhani and M. Patzold, "A unified disk scattering model and its angle-of-departure and time-of-arrival statistics," *Vehicular Technology, IEEE Transactions on*, vol. 62, pp. 473–485, Feb 2013.

[59] M. Patzold and B. Hogstad, "A space-time channel simulator for mimo channels based on the geometrical one-ring scattering model," in *Vehicular Technology Conference, 2004. VTC2004-Fall. 2004 IEEE 60th*, vol. 1, pp. 144–149 Vol. 1, Sept 2004.

[60] A. Abdi and M. Kaveh, "A space-time correlation model for multielement antenna systems in mobile fading channels," *Selected Areas in Communications, IEEE Journal on*, vol. 20, pp. 550–560, Apr 2002.

[61] D. Van Rheeden and S. Gupta, "A geometric model for fading correlation in multipath radio channels," in *Communications, 1998. ICC 98. Conference Record. 1998 IEEE International Conference on*, vol. 3, pp. 1655–1659 vol.3, Jun 1998.

[62] P. Petrus, J. Reed, and T. Rappaport, "Geometrically based statistical channel model for macrocellular mobile environments," in *Global Telecommunications Conference, 1996. GLOBECOM '96. 'Communications: The Key to Global Prosperity*, vol. 2, pp. 1197–1201 vol.2, Nov 1996.

[63] I. Jaafar, H. Boujemaa, and M. Siala, "Angle and time of arrival statistics for hollow-disc and elliptical scattering models," in *Signals, Circuits and Systems, 2008. SCS 2008. 2nd International Conference on*, pp. 1–4, Nov 2008.

[64] A. Borhani and M. Patzold, "Time-of-arrival, angle-of-arrival, and angle-of-departure statistics of a novel simplistic disk channel model," in *Signal Processing and Communication Systems (ICSPCS), 2011 5th International Conference on*, pp. 1–7, Dec 2011.

[65] P. Almers, F. Tufvesson, and A. Molisch, "Keyhole effect in mimo wireless channels: Measurements and theory," *Wireless Communications, IEEE Transactions on*, vol. 5, pp. 3596–3604, December 2006.

العنوان:	-Realistic Modeling of Time-Varying MIMO Channel Capacity Using Ray Tracing in Multi-Ring Scattering Environment
المؤلف الرئيسي:	Shtaiwi, Eyad Mahmoud
مؤلفين آخرين:	Harb, Bassam(Advisor)
التاريخ الميلادي:	2015
موقع:	إربد
الصفحات:	1 - 64
رقم MD:	747732
نوع المحتوى:	رسائل جامعية
اللغة:	English
الدرجة العلمية:	رسالة ماجستير
الجامعة:	جامعة اليرموك
الكلية:	كلية الحجاوي للهندسة التكنولوجية
الدولة:	الاردن
قواعد المعلومات:	Dissertations
مواضيع:	أنظمة الاتصالات اللاسلكية
رابط:	https://search.mandumah.com/Record/747732

Appendix A

APPENDEX A

$$h_{m,n}(t) = \sum_{l=1}^{K-1} A_l e^{j\psi_l} e^{-j2\pi f_c \tau_l(t)} e^{j\vec{k}_M^l . \vec{x}_M^m + j\vec{k}_B^l . \vec{x}_B^n} \tag{A.1}$$

The covariance of MIMO channel is computed as [57]:

$$\Sigma_H = E\{vec(\mathbf{H}) \otimes vec(\mathbf{H}^H)\} \tag{A.2}$$

For Time-varying flat-fading MIMO channel gains matrix $\mathbf{H}$ is written as:

$$\mathbf{H}(t) = \begin{bmatrix} h_{1,1}(t) & h_{1,2}(t) & \dots & h_{1,N}(t) \\ h_{2,1}(t) & h_{2,2}(t) & \dots & h_{2,N}(t) \\ \vdots & \ddots & \ddots & \vdots \\ h_{M,1}(t) & h_{M,2}(t) & \dots & h_{M,N}(t) \end{bmatrix} \tag{A.3}$$

The correlation between the channel at instant t and instant $t+\Delta t$ is given by:

$$R(t, t+\Delta t) = \mathrm{E}\left\{vec(\mathbf{H}(t)) \otimes \left(\mathbf{H}^H(t+\Delta t)\right)\right\} \tag{A.4}$$

$$\mathbf{H}^H(t+\Delta t) = \begin{bmatrix} h_{1,1}^*(t+\Delta t) & h_{2,1}^*(t+\Delta t) & \dots & h_{M,1}^*(t+\Delta t) \\ h_{1,2}^*(t+\Delta t) & h_{2,2}^*(t+\Delta t) & \dots & h_{M,2}^*(t+\Delta t) \\ \vdots & \ddots & \ddots & \vdots \\ h_{1,N}^*(t+\Delta t) & h_{2,N}^*(t+\Delta t) & \dots & h_{M,N}^*(t+\Delta t) \end{bmatrix} \tag{A.5}$$

$$R(t,t+\Delta t)=\begin{bmatrix} \mathrm{E}\left\{h_{1,1}(t)h^*_{1,1}(t+\Delta t)\right\} & \mathrm{E}\left\{h_{1,2}(t)h^*_{2,1}(t+\Delta t)\right\} & \dots & \mathrm{E}\left\{h_{1,N}(t)h^*_{M,1}(t+\Delta t)\right\} \\ \mathrm{E}\left\{h_{2,1}(t)h^*_{1,2}(t+\Delta t)\right\} & \mathrm{E}\left\{h_{2,2}(t)h^*_{2,2}(t+\Delta t)\right\} & \dots & \mathrm{E}\left\{h_{2,N}(t)h^*_{M,2}(t+\Delta t)\right\} \\ \vdots & \ddots & \ddots & \vdots \\ \mathrm{E}\left\{h_{M,1}(t)h^*_{1,N}(t+\Delta t)\right\} & \mathrm{E}\left\{h_{M,2}(t)h^*_{2,N}(t+\Delta t)\right\} & \dots & \mathrm{E}\left\{h_{M,N}(t)h^*_{M,N}(t+\Delta t)\right\} \end{bmatrix} \tag{A.6}$$

To get $\mathrm{E}\left\{h_{p,r}(t)h^*_{q,s}(t+\Delta t)\right\}$, We need to expand the summation in A.1. So,

$$\begin{aligned} h_{p,r}(t) = {} & A_0 e^{j\psi_o} e^{-j2\pi f_c \tau_o(t)} e^{j\vec{k}^o_M.\vec{x}^p_M + j\vec{k}^o_B.\vec{x}^r_B} + A_1 e^{j\psi_1} e^{-j2\pi f_c \tau_1(t)} e^{j\vec{k}^1_M.\vec{x}^p_M + j\vec{k}^1_B.\vec{x}^r_B} + \dots \\ & + A_{K-1} e^{j\psi_{K-1}} e^{-j2\pi f_c \tau_{K-1}(t)} e^{j\vec{k}^{K-1}_M.\vec{x}^p_M + j\vec{k}^{K-1}_B.\vec{x}^r_B} \end{aligned} \tag{A.7}$$

And

$$\begin{aligned} h^*_{q,s}(t+\Delta t) = {} & A^*_0 e^{-j\psi_o} e^{j2\pi f_c \tau_o(t+\Delta t)} e^{-j\vec{k}^o_M.\vec{x}^q_M - j\vec{k}^o_B.\vec{x}^s_B} + A^*_1 e^{-j\psi_1} e^{j2\pi f_c \tau_1(t+\Delta t)} e^{-j\vec{k}^1_M.\vec{x}^q_M - j\vec{k}^1_B.\vec{x}^s_B} + \dots \\ & + A^*_{K-1} e^{-j\psi_{K-1}} e^{j2\pi f_c \tau_{K-1}(t+\Delta t)} e^{-j\vec{k}^{K-1}_M.\vec{x}^q_M - j\vec{k}^{K-1}_B.\vec{x}^s_B} \end{aligned} \tag{A.8}$$

$$\begin{aligned} & h_{p,r}(t)h^*_{q,s}(t+\Delta t) = A_0 A^*_0 e^{j\psi_o} e^{-j\psi_o} e^{-j2\pi f_c \tau_o(t)} e^{j2\pi f_c \tau_o(t+\Delta t)} e^{j\vec{k}^o_M.\vec{x}^p_M + j\vec{k}^o_B.\vec{x}^r_B} e^{-j\vec{k}^o_M.\vec{x}^q_M - j\vec{k}^o_B.\vec{x}^s_B} + \\ & A_0 A^*_1 e^{j\psi_o} e^{-j\psi_1} e^{-j2\pi f_c \tau_o(t)} e^{j2\pi f_c \tau_1(t+\Delta t)} e^{j\vec{k}^o_M.\vec{x}^p_M + j\vec{k}^o_B.\vec{x}^r_B} e^{-j\vec{k}^1_M.\vec{x}^q_M - j\vec{k}^1_B.\vec{x}^s_B} + \dots + \\ & A_{K-1} A^*_{K-1} e^{j\psi_{K-1}} e^{-j\psi_{K-1}} e^{-j2\pi f_c \tau_{K-1}(t)} e^{j2\pi f_c \tau_{K-1}(t+\Delta t)} e^{j\vec{k}^{K-1}_M.\vec{x}^p_M + j\vec{k}^{K-1}_B.\vec{x}^r_B} e^{-j\vec{k}^{K-1}_M.\vec{x}^q_M - j\vec{k}^{K-1}_B.\vec{x}^s_B} \end{aligned} \tag{A.9}$$

$$\begin{aligned} h_{p,r}(t)h^*_{q,s}(t+\Delta t) = {} & A^2_0 \cancel{e^{j\psi_o} e^{-j\psi_o}} e^{-j2\pi f_c(\tau_o(t)-\tau_o(t+\Delta t))} e^{j\vec{k}^o_M.(\vec{x}^p_M - \vec{x}^q_M) + j\vec{k}^o_B.(\vec{x}^r_B - \vec{x}^s_B)} + \\ & A_0 A^*_1 e^{j\psi_o} e^{-j\psi_1} e^{-j2\pi f_c(\tau_o(t)-\tau_1(t+\Delta t))} e^{j\vec{k}^o_M.\vec{x}^p_M + j\vec{k}^o_B.\vec{x}^r_B} e^{-j\vec{k}^1_M.\vec{x}^q_M - j\vec{k}^1_B.\vec{x}^s_B} + \dots + \\ & A^2_{K-1} \cancel{e^{j\psi_{K-1}} e^{-j\psi_{K-1}}} e^{-j2\pi f_c(\tau_{K-1}(t)-\tau_{K-1}(t+\Delta t))} e^{j\vec{k}^{K-1}_M.(\vec{x}^p_M - \vec{x}^q_M) + j\vec{k}^{K-1}_B.(\vec{x}^r_B - \vec{x}^s_B)} \end{aligned} \tag{A.10}$$

The phases ψ_n and ψ_m are assumed to be independent and uniformly distributed on $U(-\pi,\pi)$. So,

$$f(\psi_n,\psi_m) = f(\psi_n)f(\psi_m) \tag{A.11}$$

And ,

$$\begin{aligned}
\mathrm{E}\left\{h_{p,r}(t)h^*_{q,s}(t+\Delta t)\right\} = \mathrm{E}\left\{A_0^2\, e^{-j2\pi f_c(\tau_o(t)-\tau_o(t+\Delta t))} e^{j\vec{k}^o_M.(\vec{x}^p_M-\vec{x}^q_M)+j\vec{k}^o_B.(\vec{x}^r_B-\vec{x}^s_B)}\right\} + \\
\mathrm{E}\left\{A_0A_1^* e^{j\psi_o} e^{-j\psi_1} e^{-j2\pi f_c(\tau_o(t)-\tau_1(t+\Delta t))} e^{j\vec{k}^o_M.\vec{x}^p_M+j\vec{k}^o_B.\vec{x}^r_B} e^{-j\vec{k}^1_M.\vec{x}^q_M-j\vec{k}^1_B.\vec{x}^s_B}\right\} + \\
\ldots + \mathrm{E}\left\{A_nA_m^* e^{j\psi_n} e^{-j\psi_m} e^{-j2\pi f_c(\tau_n(t)-\tau_m(t+\Delta t))} e^{j\vec{k}^n_M.\vec{x}^p_M+j\vec{k}^n_B.\vec{x}^r_B} e^{-j\vec{k}^m_M.\vec{x}^q_M-j\vec{k}^m_B.\vec{x}^s_B}\right\} + \ldots \\
+ \mathrm{E}\left\{A_{K-1}^2\, e^{-j2\pi f_c(\tau_{K-1}(t)-\tau_{K-1}(t+\Delta t))} e^{j\vec{k}^{K-1}_M.(\vec{x}^p_M-\vec{x}^q_M)+j\vec{k}^{K-1}_B.(\vec{x}^r_B-\vec{x}^s_B)}\right\}
\end{aligned} \tag{A.12}$$

$$\begin{aligned}
&\mathrm{E}\left\{A_nA_m^* e^{j\psi_n} e^{-j\psi_m} e^{-j2\pi f_c(\tau_n(t)-\tau_m(t+\Delta t))} e^{j\vec{k}^n_M.\vec{x}^p_M+j\vec{k}^n_B.\vec{x}^r_B} e^{-j\vec{k}^m_M.\vec{x}^q_M-j\vec{k}^m_B.\vec{x}^s_B}\right\} = \\
&\int_{\psi_n=-\pi}^{\pi}\int_{\psi_m=-\pi}^{\pi} f(\psi_{\mathbf{n}},\psi_{\mathbf{m}}) A_nA_m^* e^{j\psi_n} e^{-j\psi_m} e^{-j2\pi f_c(\tau_n(t)-\tau_m(t+\Delta t))} e^{j\vec{k}^n_M.\vec{x}^p_M+j\vec{k}^n_B.\vec{x}^r_B} e^{-j\vec{k}^m_M.\vec{x}^q_M-j\vec{k}^m_B.\vec{x}^s_B}\, d\psi_n\, d\psi_m \\
&= A_nA_m^* e^{-j2\pi f_c(\tau_n(t)-\tau_m(t+\Delta t))} e^{j\vec{k}^n_M.\vec{x}^p_M+j\vec{k}^n_B.\vec{x}^r_B} e^{-j\vec{k}^m_M.\vec{x}^q_M-j\vec{k}^m_B.\vec{x}^s_B} \int_{-\pi}^{\pi} f(\psi_{\mathbf{n}}) e^{j\psi_n} d\psi_n \int_{-\pi}^{\pi} f(\psi_{\mathbf{m}}) e^{j\psi_m} d\psi_m \\
&= A_nA_m^* e^{-j2\pi f_c(\tau_n(t)-\tau_m(t+\Delta t))} e^{j\vec{k}^n_M.\vec{x}^p_M+j\vec{k}^n_B.\vec{x}^r_B} e^{-j\vec{k}^m_M.\vec{x}^q_M-j\vec{k}^m_B.\vec{x}^s_B} \underbrace{\int_{-\pi}^{\pi} \frac{1}{2\pi} e^{j\psi_n} d\psi_n}_{I_1} \underbrace{\int_{-\pi}^{\pi} \frac{1}{2\pi} e^{j\psi_m} d\psi_m}_{I_2}
\end{aligned} \tag{A.13}$$

$$\begin{aligned}
I_1 = I_2 &= \frac{e^{j\psi_n}}{2\pi j}\Big|_{-\pi}^{\pi} \\
&= \frac{e^{j\pi} - e^{-j\pi}}{2\pi j} \\
&= \frac{\sin(\pi)}{\pi} = 0
\end{aligned} \tag{A.14}$$

Equation A.13 equal to zero when $n \neq m$. and equation A.12 becomes :

$$\begin{aligned}
\mathrm{E}\left\{h_{p,r}(t)h^*_{q,s}(t+\Delta t)\right\} = \mathrm{E}\left\{A_0^2\, e^{-j2\pi f_c(\tau_o(t)-\tau_o(t+\Delta t))} e^{j\vec{k}^o_M.(\vec{x}^p_M-\vec{x}^q_M)+j\vec{k}^o_B.(\vec{x}^r_B-\vec{x}^s_B)}\right\} + \\
\mathrm{E}\left\{A_1^2\, e^{-j2\pi f_c(\tau_1(t)-\tau_1(t+\Delta t))} e^{j\vec{k}^1_M.(\vec{x}^p_M-\vec{x}^q_M)+j\vec{k}^1_B.(\vec{x}^r_B-\vec{x}^s_B)}\right\} + \ldots \\
\ldots + \mathrm{E}\left\{A_m^2\, e^{-j2\pi f_c(\tau_m(t)-\tau_m(t+\Delta t))} e^{j\vec{k}^m_M.(\vec{x}^p_M-\vec{x}^q_M)+j\vec{k}^m_B.(\vec{x}^r_B-\vec{x}^s_B)}\right\} + \ldots \\
+ \mathrm{E}\left\{A_{K-1}^2\, e^{-j2\pi f_c(\tau_{K-1}(t)-\tau_{K-1}(t+\Delta t))} e^{j\vec{k}^{K-1}_M.(\vec{x}^p_M-\vec{x}^q_M)+j\vec{k}^{K-1}_B.(\vec{x}^r_B-\vec{x}^s_B)}\right\}
\end{aligned} \tag{A.15}$$

Equation A.15 can be rewriten as:

$$\mathrm{E}\left\{h_{p,r}(t)h^{*}_{q,s}(t+\Delta t)\right\} = \mathrm{E}\left\{\sum_{m=0}^{K-1} A_m^2\, e^{-j2\pi f_c(\tau_m(t)-\tau_m(t+\Delta t))} e^{j\vec{k}_M^m.(\vec{x}_M^p-\vec{x}_M^q)+j\vec{k}_B^m.(\vec{x}_B^r-\vec{x}_B^s)}\right\} \tag{A.16}$$

Where the path delay for m^{th} path is given by:

$$\tau_m(t) \approx \tau_m^0 + \frac{|\vec{v}|t}{c}\cos\alpha_m \tag{A.17}$$

Then $\tau_m(t) - \tau_m(t+\Delta t)$ is calculated as:

$$\begin{aligned}\tau_m(t) - \tau_m(t+\Delta t) \approx& \tau_m^0 + \frac{|\vec{v}|t}{c}\cos\alpha_m - \left(\tau_m^0 + \frac{|\vec{v}|(t+\Delta t}{c}\cos\alpha_m\right)\\ \approx& \frac{-|\vec{v}|\Delta t}{c}\cos\alpha_m\end{aligned} \tag{A.18}$$

Substituting equation A.18 in equation A.16 we get:

$$\mathrm{E}\left\{h_{p,r}(t)h^{*}_{q,s}(t+\Delta t)\right\} = \mathrm{E}\left\{\sum_{m=0}^{K-1} A_m^2\, e^{j2\pi f_c(\frac{|\vec{v}|\Delta t}{c}\cos\alpha_m)} e^{j\vec{k}_M^m.(\vec{x}_M^p-\vec{x}_M^q)+j\vec{k}_B^m.(\vec{x}_B^r-\vec{x}_B^s)}\right\} \tag{A.19}$$

From the figure above :

$$\begin{aligned}\vec{x}_B^r - \vec{x}_B^s =& (-d_0\cos\gamma_{rs}\,\hat{a}_x + d_0\sin\gamma_{rs}\,\hat{a}_y) - (-(d_{rs}+d_0)\cos\gamma_{rs}\,\hat{a}_x + (d_{rs}+d_0)\sin\gamma_{rs}\,\hat{a}_y)\\ =& d_{rs}\cos\gamma_{rs}\,\hat{a}_x - d_{rs}\sin\gamma_{rs}\,\hat{a}_y\end{aligned} \tag{A.20}$$

Where : d_{rs} is the distance between r^{th} and s^{th} elements on the array at the basestation. And γ_{rs} is the angle between the $x-$axis and the line that joins the elements at the array. So, equation A.20 is written as:

$$\vec{x}_B^r - \vec{x}_B^s = d_{rs}(\cos\gamma_{rs}, \sin\gamma_{rs}, 0) \tag{A.21}$$

Figure A.1: Antenna Configuration at BS

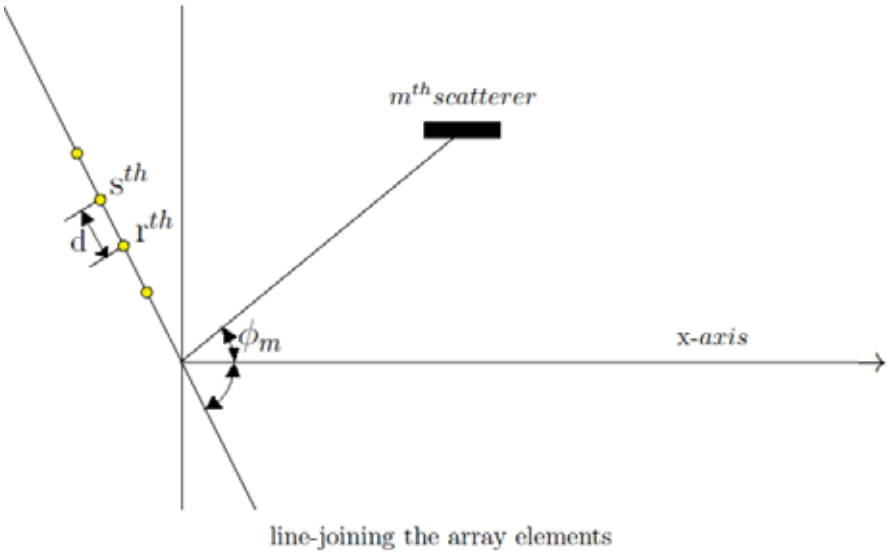

Following the same procedures $\vec{x}_M^p - \vec{x}_M^q$ is written as:

$$\vec{x}_M^p - \vec{x}_M^q = D_{pq}(\cos\Gamma_{pq}, \sin\Gamma_{pq}, 0) \tag{A.22}$$

Where : D_{pq} is the distance between q^{th} and p^{th} elements on the array at the mobile.

And Γ_{pq} is the angle between the $x-$axis and the line that joins the elements on the array at the mobile.

So,

$$\begin{aligned}\vec{k}_B^m \cdot (\vec{x}_B^r - \vec{x}_B^s) &= \frac{2\pi}{\lambda}(\cos\phi_m, \sin\phi_m, 0) \cdot d_{rs}(\cos\gamma_{rs}, \sin\gamma_{rs}, 0) \\ &= \frac{2\pi d_{rs}}{\lambda}(\cos\phi_m\cos\gamma_{rs} + \sin\phi_m\sin\gamma_{rs}) \\ &= \frac{2\pi d_{rs}}{\lambda}\cos(\phi_m - \gamma_{rs})\end{aligned} \tag{A.23}$$

Using the Identity: $\cos(X-Y) = \cos X \cos Y + \sin X \sin Y$

Referring to Figure 4.1 and following same approach in A.23

$$\begin{aligned}\vec{k}_M^m \cdot (\vec{x}_M^p - \vec{x}_B^q) &= \frac{2\pi}{\lambda}(\cos\theta_m, \sin\theta_m, 0) \cdot D_{pq}(\cos\Gamma_{pq}, \sin\Gamma_{pq}, 0) \\ &= \frac{2\pi D_{pq}}{\lambda}(\cos\theta_m \cos\Gamma_{pq} + \sin\theta_m \sin\Gamma_{pq}) \\ &= \frac{2\pi D_{pq}}{\lambda}\cos(\theta_m - \Gamma_{pq})\end{aligned} \tag{A.24}$$

Substitute (A.23)and (1.27) in (A.19) and maximum Doppler spread formula, $f_d = \frac{fc.|\vec{v}|}{c}$ we get:

$$\mathrm{E}\left\{h_{p,r}(t)h^*_{q,s}(t+\Delta t)\right\} = \mathrm{E}\left\{\sum_{m=0}^{K-1} A_m^2\, e^{j2\pi f_d \Delta t \cos\alpha_m} e^{\frac{j2\pi d_{rs}}{\lambda}\cos(\phi_m - \gamma_{rs})}\, e^{j\frac{2\pi D_{pq}}{\lambda}\cos(\theta_m - \Gamma_{pq})}\right\} \tag{A.25}$$

Refering to the geometry in Figure A.1, $\angle\alpha_m = \pi - (\angle\theta_m - \angle\gamma)$ So,

$$\cos\alpha_m = -\cos(\theta_m - \gamma) \tag{A.26}$$

subsitute A.26 in A.25 we get:

$$\begin{aligned}
&\mathrm{E}\left\{h_{p,r}(t)h^{*}_{q,s}(t+\Delta t)\right\} = \mathrm{E}\left\{\sum_{m=0}^{K-1} A_m^2\; e^{j2\pi f_d \Delta t \cos(\theta_{\mathbf{m}}-\gamma)} e^{j\frac{2\pi d_{rs}}{\lambda}\cos(\phi_m-\gamma_{rs})}\; e^{j\frac{2\pi D_{pq}}{\lambda}\cos(\theta_m-\Gamma_{pq})}\right\} \\
&= \mathrm{E}\left\{\sum_{m=0}^{K-1} A_m^2\; e^{-j2\pi\left(f_d\Delta t\cos(\theta_m-\gamma)+\frac{D_{pq}}{\lambda}\cos(\theta_m-\Gamma_{pq})\right)} e^{j\frac{2\pi d_{rs}}{\lambda}\cos(\phi_m-\gamma_{rs})}\right\} \\
&= \mathrm{E}\left\{\sum_{m=0}^{K-1} A_m^2 e^{-j2\pi\left[f_d\Delta t(\cos\theta_m\cos\gamma+\sin\theta_m\sin\gamma)+\frac{D_{pq}}{\lambda}(\cos\theta_m\cos\Gamma_{pq}+\sin\theta_m\sin\Gamma_{pq})\right]} e^{j\frac{2\pi d_{rs}}{\lambda}\cos(\phi_m-\gamma_{rs})}\right\} \\
&= \mathrm{E}\left\{\sum_{m=0}^{K-1} A_m^2 e^{-j2\pi\left[\cos\theta_m\left(f_d\Delta t\cos\gamma-\frac{D_{pq}}{\lambda}\cos\Gamma_{pq}\right)+\sin\theta_m\left(f_d\Delta t\sin\gamma-\frac{D_{pq}}{\lambda}\sin\Gamma_{pq}\right)\right]} e^{j\frac{2\pi d_{rs}}{\lambda}\cos(\phi_m-\gamma_{rs})}\right\}
\end{aligned} \tag{A.27}$$

Special case, θ_m is assumed to be uniformly distributed on $(-\pi,\pi)$. And θ_n, θ_m are independent for different scatterers. So,

$$\begin{aligned}
&\mathrm{E}_{\theta_m}\left\{A_m^2 e^{-j2\pi\left[\cos\theta_m\left(f_d\Delta t\cos\gamma-\frac{D_{pq}}{\lambda}\cos\Gamma_{pq}\right)+\sin\theta_m\left(f_d\Delta t\sin\gamma-\frac{D_{pq}}{\lambda}\sin\Gamma_{pq}\right)\right]} e^{j\frac{2\pi d_{rs}}{\lambda}\cos(\phi_m-\gamma_{rs})}\right\} \\
&= A_m^2 e^{j\frac{2\pi d_{rs}}{\lambda}\cos(\phi_m-\gamma_{rs})}\mathrm{E}_{\theta_m}\left\{e^{-j2\pi\left[\cos\theta_m\left(f_d\Delta t\cos\gamma-\frac{D_{pq}}{\lambda}\cos\Gamma_{pq}\right)+\sin\theta_m\left(f_d\Delta t\sin\gamma-\frac{D_{pq}}{\lambda}\sin\Gamma_{pq}\right)\right]}\right\} \\
&= A_m^2 e^{j\frac{2\pi d_{rs}}{\lambda}\cos(\phi_m-\gamma_{rs})}\left(\int_{-\pi}^{\pi}\frac{1}{2\pi}e^{-j2\pi\left[\cos\theta_m\left(f_d\Delta t\cos\gamma-\frac{D_{pq}}{\lambda}\cos\Gamma_{pq}\right)+\sin\theta_m\left(f_d\Delta t\sin\gamma-\frac{D_{pq}}{\lambda}\sin\Gamma_{pq}\right)\right]}\right)
\end{aligned} \tag{A.28}$$

Using the fact :

$$\frac{1}{2\pi}\int_{-\pi}^{\pi}\exp\left(a\cos x+b\sin x\right)dx = J_0\left(\sqrt{a^2+b^2}\right) \tag{A.29}$$

Then, (A.28) becomes:

$$\begin{aligned}
&A_m^2 e^{j\frac{2\pi d_{rs}}{\lambda}\cos(\phi_m-\gamma_{rs})}\left(\int_{-\pi}^{\pi}\frac{1}{2\pi}e^{-j2\pi\left[\cos\theta_m\left(f_d\Delta t\cos\gamma-\frac{D_{pq}}{\lambda}\cos\Gamma_{pq}\right)+\sin\theta_m\left(f_d\Delta t\sin\gamma-\frac{D_{pq}}{\lambda}\sin\Gamma_{pq}\right)\right]}\right) = \\
&A_m^2 e^{j\frac{2\pi d_{rs}}{\lambda}\cos(\phi_m-\gamma_{rs})}J_0\left(2\pi\sqrt{\left(f_d\Delta t\cos\gamma-\frac{D_{pq}}{\lambda}\cos\Gamma_{pq}\right)^2+\left(f_d\Delta t\sin\gamma-\frac{D_{pq}}{\lambda}\sin\Gamma_{pq}\right)^2}\right)
\end{aligned} \tag{A.30}$$

Appendix B

APPENDEX B

The MS, Bs, and the scatterer represent vertices of triangle, Figure B.1. Using trigonometric identities we need to find the relation between AoA and AoD, $p(\theta,\phi)$.

$$L = r\sin(\pi-\theta) \tag{B.1}$$

$$\begin{aligned}\tan(\phi) &= \frac{L}{D-r\cos(\pi-\theta)} \\ &= \frac{r\sin(\pi-\theta)}{D-r\cos(\pi-\theta)}\end{aligned} \tag{B.2}$$

$$\tan(\phi) = \frac{r\sin(\theta)}{D+r\cos(\theta)} \tag{B.3}$$

Equation (B.3) can be simplified as:

$$\begin{aligned}&D\tan(\phi)+r\cos(\theta)\tan(\phi)-r\sin(\theta)=0 \\ &D\tan(\phi)+r\left(\cos(\theta)\tan(\phi)-\sin(\theta)\right)=0 \\ &D\tan(\phi)\cos(\phi)+r\left(\cos(\theta)\sin(\phi)-\sin(\theta)\cos(\phi)\right)=0\end{aligned} \tag{B.4}$$

Using:

$$\sin(\alpha-\beta)=\sin\alpha\cos\beta-\cos\alpha\sin\beta \tag{B.5}$$

Figure B.1: Triangle formed by MS, BS and scatterer used to derive joint PDF of AoA and AoD

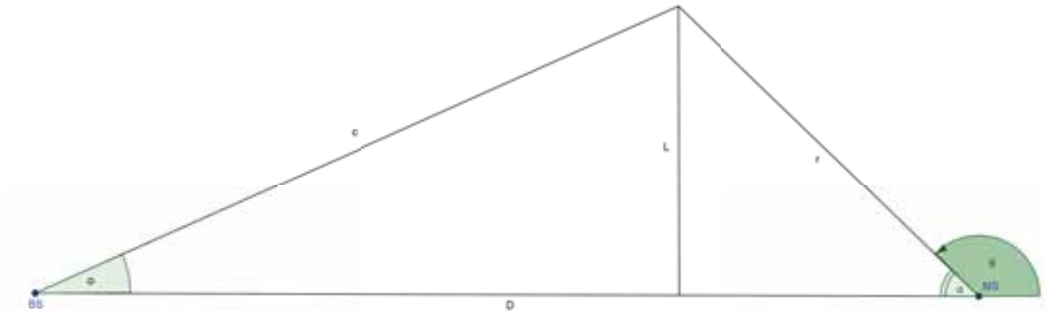

Equation B.4 becomes :

$$r=\frac{D\sin(\phi)}{\sin(\phi-\theta)} \tag{B.6}$$

The joint PDF of AoA and AoD, $p(\theta,\phi)$, can be obtained by Jacoubian transformation for Eq.(3.7):

$$p_{r,\theta}^{(k)}(r,\theta)=\begin{cases}\frac{(k+1)}{2\pi R^{k+1}}r^k & ,0\le r\le R,-\pi\le\theta\le\pi\\ 0 & ,\text{otherwise}\end{cases} \tag{B.7}$$

So,

$$p(\theta,\phi)=\frac{p_{r,\theta}\left(\frac{D\sin(\phi)}{\sin(\phi-\theta)},\theta\right)}{|J|} \tag{B.8}$$

$$|J| = \begin{vmatrix} \frac{\partial r}{\partial \phi} & \frac{\partial r}{\partial \theta} \\ \frac{\partial \theta}{\partial \phi} & \frac{\partial \theta}{\partial \theta} \end{vmatrix} \tag{B.9}$$

Where :

$$r = \frac{D\sin(\phi)}{\sin(\phi-\theta)} \tag{B.10}$$

$$|J| = \begin{vmatrix} -D\sin(\theta)\csc^2(\theta-\phi) & \frac{D\sin\phi\cos(\theta-\phi)}{\sin^2(\theta-\phi)} \\ 0 & 1 \end{vmatrix} \tag{B.11}$$

Finally

$$p(\theta,\phi) = \frac{p_{r,\theta}\left(\frac{D\sin(\phi)}{\sin(\phi-\theta)},\theta\right)}{-D\sin(\theta)\csc^2(\theta-\phi)} \tag{B.12}$$

By substituting in (B.13)

$$p^{(k)}_{r,\theta}(r,\theta) = \begin{cases} D^{k+1}\frac{(k+1)}{2\pi R^{k+1}}\frac{|\sin(\theta)|\sin^k(\phi)}{\sin^{k+2}(\theta-\phi)} & , (\phi,\theta)\in\mathcal{S} \\ 0 & , \text{otherwise} \end{cases} \tag{B.13}$$

Where:

$$\mathcal{S} \in \left\{(\phi,\theta) \mid 0 \le \frac{D\sin(\phi)}{\sin(\theta-\phi)} \le R, \theta \ne \phi\right\}$$

العنوان:	-Realistic Modeling of Time-Varying MIMO Channel Capacity Using Ray Tracing in Multi-Ring Scattering Environment
المؤلف الرئيسي:	Shtaiwi, Eyad Mahmoud
مؤلفين آخرين:	Harb, Bassam(Advisor)
التاريخ الميلادي:	2015
موقع:	إربد
الصفحات:	1 - 64
رقم MD:	747732
نوع المحتوى:	رسائل جامعية
اللغة:	English
الدرجة العلمية:	رسالة ماجستير
الجامعة:	جامعة اليرموك
الكلية:	كلية الحجاوي للهندسة التكنولوجية
الدولة:	الاردن
قواعد المعلومات:	Dissertations
مواضيع:	أنظمة الاتصالات اللاسلكية
رابط:	https://search.mandumah.com/Record/747732

YARMOUK UNIVERSITY

HIJJAWI FACULTY FOR ENGINEERING TECHNOLOGY

MASTER THESIS

Realistic Modeling of Time-Varying MIMO Channel Capacity Using Ray-Tracing in Multi-Ring Scattering Environment

Thesis Submitted to:
The Department of Telecommunications Engineering

In partial fulfilment of the requirements
for the degree of Master of Science

By:
EYAD MAHMOUD SHTAIWI
Supervisor:
DR. BASSAM HARB

April 2015